Frustrated Magnetic Interactions, Giant Magneto-Elastic Coupling, and Magnetic Phonons in Iron-Pnictides

Taner Yildirim[1,2*]
[1] *NIST Center for Neutron Research, National Institute of Standards and Technology, Gaithersburg, Maryland 20899, USA*
[2] *Department of Materials Science and Engineering, University of Pennsylvania, Philadelphia, PA 19104, USA*

(Dated: February 20, 2009)

We present a detailed first principles study of Fe-pnictides with particular emphasis on competing magnetic interactions, structural phase transition, giant magneto-elastic coupling and its effect on phonons. The exchange interactions $J_{i,j}(R)$ are calculated up to $\approx$ 12 Å from two different approaches based on direct spin-flip and infinitesimal spin-rotation. We find that $J_{i,j}(R)$ has an oscillatory character with an envelop decaying as $1/R^3$ along the stripe-direction while it is very short range along the diagonal direction and antiferromagnetic. A brief discussion of the neutron scattering determination of these exchange constants from a single crystal sample with orthorhombic twinning is given. The lattice parameter dependence of the exchange constants, $dJ_{i,j}/da$ are calculated for a simple spin-Peierls like model to explain the fine details of the tetragonal-orthorhombic phase transition. We then discuss giant magneto-elastic effects in these systems. We show that when the Fe-spin is turned off the optimized c-values are shorter than experimetnal values by 1.4 Å for $CaFe_2As_2$, by 0.4 Å for $BaFe_2As_2$, and by 0.13 Å for LaOFeAs. We explain this strange behavior by unraveling surprisingly strong interactions between arsenic ions, the strength of which is controlled by the Fe-spin state through Fe-As hybridization. Reducing the Fe-magnetic moment, weakens the Fe-As bonding, and in turn, increases As-As interactions, causing a giant reduction in the c-axis. These findings also explain why the Fe-moment is so tightly coupled to the As-z position. Finally, we show that Fe-spin is also required to obtain the right phonon energies, in particular As c-polarized and Fe-Fe in-plane modes that have been recently observed by inelastic x-ray and neutron scattering but cannot be explained based on non-magnetic phonon calculations. Since treating iron as magnetic ion always gives much better results than non-magnetic ones and since there is no large c-axis reduction during the normal to superconducting phase transition, the iron magnetic moment should be present in Fe-pnictides at all times. We discuss the implications of our results on the mechanism of superconductivity in these fascinating Fe-pnictide systems.

PACS numbers: 74.25.Jb,67.30.hj,75.30.Fv,75.25.tz,74.25.Kc

I. INTRODUCTION

The recent discovery of superconductivity at T_c's up to 55 K in iron-pnictide systems[1,2,3,4] has sparked enormous interest in this class of materials. So far four types of materials have been discovered. The first one is the rare-earth pnictide oxide layered systems, REOFeAs which is denoted as "1111"[1,2,3,4,5]. The second class is the so called "122" systems with the chemical formula MFe_2As_2 (M=Ca,Sr, etc)[5,6,7,8,9]. The third system with $T_c = 18$ K is MFeAs (M=Li and Na), which is similar to REOFeAs but instead of REO-layers, we have now small alkali metals such as Li[10]. The last one is the binary Fe(Se,Te) systems which have been shown to superconduct up to 12 K under pressure[11].

The crystal structures of these four systems are shown in Fig. 1. The common feature in these Fe-pnictide superconductors is the presence of FeAs plane (or Fe(Te,Se) in the case of 11 systems), which is shown in Fig. 2. Basically Fe atoms form a regular square lattice just like the CuO_2 plane in cuprates. However the important difference is the location of the arsenic ions which are not located between two Fe ions but rather above/below the center of Fe-square. This arrangement of arsenic ions has several important consequences in the electronic and magnetic properties of these systems. Since As is not directly between two Fe ions, the Fe-Fe distance is not large and direct Fe-Fe overlap plays an important role in the band formation near the Fermi level. Then, the delicate interplay between Fe-Fe, Fe-As, and even As-As interactions (which is very important in 122 systems such as Ca122) result interesting electronic and magnetic prop-

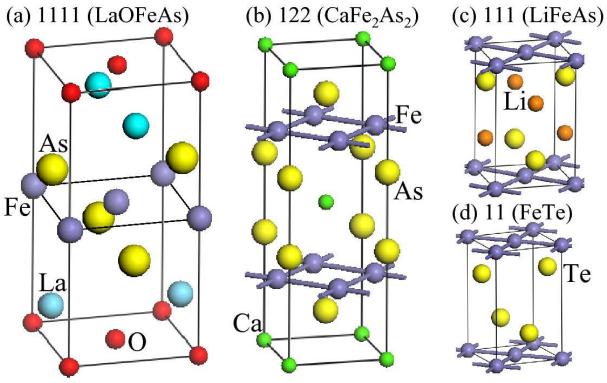

FIG. 1: (color online) The crystal structures (with origin choice 1) of four types of Fe-pnictide systems that have been discovered so far.

erties that are super-sensitive to the As-z position and the c-lattice parameter of the Fe-pnictide system. In this paper, we will focus on the structural, dynamical and magnetic properties of 1111 and 122 systems only. For a recent review of electronic and superconducting properties of Fe-based superconductors, we refer the reader to David Singh's[12] and Igor Mazin's[13] articles in this issue and references therein.

A common phase diagram for iron-pnictides has emerged[14] in which the stoichiometric parent compound shows a structural anomaly around 150-200 K, below which spin-density-wave (SDW) antiferromagnetic ordering[6,7,8,15,16] appears, which is due to nesting Fermi surfaces[17,18,19,20]. The SDW ordering is further stabilized against the normal checkerboard antiferromagnetic ordering (denoted as AF1) due to strong antiferromagnetic interactions along the Fe-square diagonal[21]. Superconductivity in these systems only occurs when the SDW ordering and the structural distortion are suppressed, which can be achieved in a number of ways such as fluorine doping on the oxygen site[1,2,3,4], or hole doping ($La_{1-x}Sr_x$)[22,23,24,25] or by applying external pressure[26,27,28].

The structural distortion which is common to all parent compounds can be characterized by either primitive monoclinic space group P2/c (P112/n) or the conventional orthorhombic cell with space group Cmma[29]. The relation of these two representations is indicated in the bottom panel of Fig. 2. We note that when the system is distorted (i.e. $\gamma \neq 90.0$) one of the Fe-pairs gets closer and the other Fe-Fe distance gets longer, yielding an orthorhombic lattice (i..e $a_o \neq b_o$). Below we will successfully explain how this structural phase transition is tightly coupled to the magnetic SDW ordering. Finally we note that the reported space groups in the SDW state[15,29] (i.e. Cmma or P2/c) are actually the space groups of the system without the Fe-magnetic moment. Hence technically the Cmma is not the right space group for the SDW magnetic system. If we ignore the antiferromagnetic stacking of the FeAs planes, the actual space group is Pbnm which is primitive as expected. This will be important in the discussion of magnetic phonon calculations in Sec. VI where we can not use the space group Cmma but has to use Pbmb for 1111 systems. The situation is very similar for the 122, 111, and 11 systems as well. For example, the Fmmm space group of 111-systems is actually reduced to Bbmb (spg. number=66, origin 1) when the iron-spins are considered.

Clearly, the understanding of electronic, magnetic, and structural properties of the parent FeAs compound is the key to determining the underlying mechanism that makes these materials superconduct upon electron/hole doping. In this paper we present a detailed first-principles study of Fe-pnictides with main focus on the competing magnetic spin-interactions, structural phase transition, the giant magneto-elastic coupling and the phonons. Our main objective is to demonstrate that Fe-spin is the key in understanding many properties of these systems, including lattice parameters, atomic positions, and the phonon spectrum. When the Fe-spin is ignored and non-magnetic calculations are done, the results do not agree with most of the experimental data. This observation could be the key in identifying the mechanism of superconductivity in these systems.

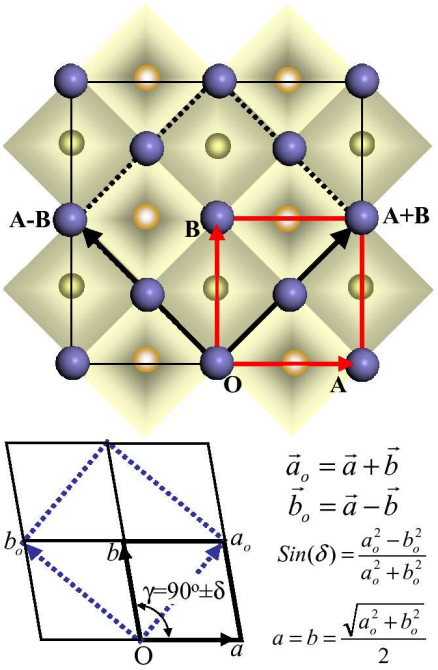

FIG. 2: (color online) Top: A view along c-axis of the FeAs-plane and the relations between the primitive and $\sqrt{2} \times \sqrt{2}$ supercell used in our calculations. The dark and light shaded areas indicate the As atoms below and above the Fe-square lattice, respectively. Bottom: Relation between conventional (Cmma) and primitive (P2/c) cells of the orthorhombic structure.

This paper is organized as follows. In the next section, we discuss the energetics of possible spin configurations in Fe-pnictides within a unified model from all-electron fix-spin moment calculations. We will show that the SDW magnetic ordering is the only stable ground state for Fe-pnictide. In Sec. III, we will calculate the exchange interactions $J_{i,j}(R)$ up to $\approx 12\mathring{A}$ using two different approaches based on direct spin-flip and infinitesimal spin-rotation. We find that $J_{i,j}(R)$ has an oscillatory character with an envelop decaying as $1/R^3$ along the stripe-directions. On the other hand, it is short range along the diagonal direction and antiferromagnetic, suggesting it is superexchange type and an important contributer towards the stabilization of SDW ordering. A brief discussion of the experimental determination of these exchange constants from an orthorhombic-twin crystal is also given in this section. In Sec. IV, we will discuss the tetragonal-orthorhombic lattice distortion. We will calculate the lattice parameter dependence of the exchange constants, $dJ_{i,j}/da$, and then use it in a simple

spin-Peierls like model to explain the fine details of the tetragonal-orthorhombic phase transition that is driven by the SDW ordering. In Sec. V, we will discuss the giant magneto-elastic effects in these systems where iron-spin controls the strength of Fe-As and As-As hybridization which results huge dependence of the magnetic and structural properties on the As-z and c-axis of the lattice. Finally, in Sec. VI, we show that Fe-spin is also required to obtain the right phonon energies, in particular As c-polarized and Fe-Fe in-plane modes that have been recently observed by inelastic x-ray and neutron scattering measurements but could not been explained based on non-magnetic phonon calculations. Our conclusions will be given in Sec. VII.

II. SPIN DENSITY WAVE (SDW) ORDERING

The early theoretical studies identified several candidate ground states for Fe-pnictides such as a non-magnetic metal near a ferromagnetic or antiferromagnetic instability[17,30,31] and a simple antiferromagnetic semi-metal[32,33]. The later calculations suggested that Fe-pnictide has an antiferromagnetic spin-density-wave (SDW) ground state[18] that is stabilized by Fermi-surface nesting[19,20] as well as by strong antiferromagnetic spin interactions along the Fe-square diagonal[21,34]. Recently several nice review articles have been published[35,36] about the Fermi surface nesting, band structure properties, and the delicate interplay between the structural and electronic properties[36] in these fascinating systems. Hence, here we will not discuss the Fermi-surface nesting and band structure properties but rather focus on the energetics of different spin-configurations in order to determine the nature of magnetic interactions present in these systems.

In order to demonstrate the SDW ground state of Fe-pnictide systems, one needs to consider $\sqrt{2}\times\sqrt{2}$ supercell of the tetragonal cell shown in Fig. 2 with four different magnetic spin configurations. These are non-magnetic (NM, i.e. no spin polarization), ferromagnetic (F) and the two different antiferromagnetic spin configurations shown in Fig. 3. The first one of the antiferromagnetic configurations is AF1 where the nearest neighbor spins are anti-parallel to each other. The second antiferromagnetic configuration, AF2, is shown in Fig. 3c and 3d. In AF2 the Fe spins along the square diagonal are aligned antiferromagnetically. This is the stripe-phase which was first predicted from Fermi-surface nesting[19,20]. The AF2 spin configuration can be considered as two interpenerating simple square AF sublattices (circle and square sublattices in Fig. 3c). From the classical Heisenberg energies of AF1 and AF2, one sees that the AF2 spin configuration is stabilized when $J_2 > J_1/2$. We note that in AF2 spin configuration, due to large antiferromagnetic J_2 interactions, the spins along the diagonal direction are aligned antiferromagnetically, forcing spins to be parallel and antiparallel along the $a-$ and $b-$directions. Hence

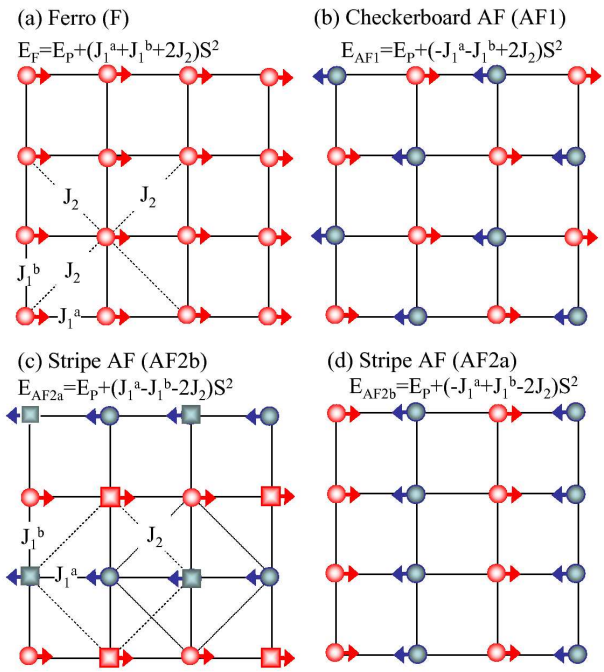

FIG. 3: (color online) Four possible magnetic configurations for the Fe-square in Fe-pnictide and the corresponding energy expressions in terms of a simple J_1^a-J_1^b-J_2 model. Two antiferromagnetic configurations are considered in this study. Top-right panel (b) shows the AF1 configuration where nearest neighbor spins are always aligned anti-parallel. Two bottom panels (c-d) show the AF2 configuration where the next nearest neighbor spins (i.e., J_2) are always aligned anti-parallel. Note that this is the same stripe-phase predicted from Fermi-surface nesting[19,20] and it is frustrated.

the J_1 interaction can not be fully satisfied and therefore the system is called frustrated. In frustrated magnetic systems, it is known that the frustration is usually removed by either a structural distortion or by other effective spin-spin interactions that originate from thermal and quantum fluctuations of the spins[37,38]. As we shall see below, in Fe-pnictide the Heisenberg picture is only an approximate model. The exchange interactions depend on the spin-configurations considered and therefore J_1^b could be even ferromagnetic in AF2, removing the frustration totally. Finally it has been recently shown that the total energy of the AF2 spin configuration increases as $\sin(\theta)^2$ when the two interpenetrating AFM sublattices are rotated by an angle θ with respect to each other[39]. Hence the infinite degeneracy of the classical Heisenberg model of AF2 structure has been already removed by either non-Heisenberg like interactions and/or long range interactions that are present in Fe-pnictides.

In order to determine which spin configurations among NM, F, AF1, and AF2, is the ground state, we have carried out total energy calculations for each case using experimental structure. The calculations were done using the full-potential linearized augmented plane-wave (FP-LAPW) method, within local density approximation

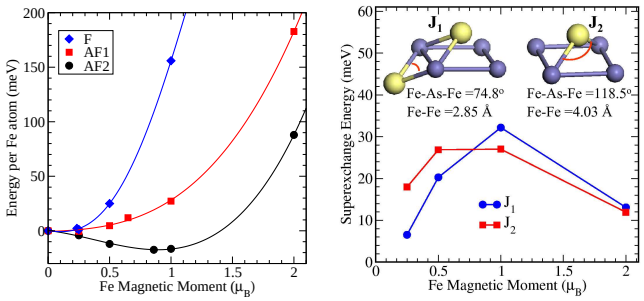

FIG. 4: (color online) (a) The total energy per Fe atom versus magnetic moment for F, AF1 and AF2 spin-configuration, indicating AF2 is the only ground state of the system. (b) The magnetic interactions for nn and nnn Fe ions obtained from the energies of F, AF, and AF2 configurations.

(LDA) using Perdew-Wang/Ceperlye-Alder exchange-correlation[40,41]. We also used the ultrasoft pseudo potential planewave (PW) method[42] for cross checking of our results and for phonon calculations. Since in spin-polarized calculations it is very easy to get a local minimum, we followed a different strategy. In our calculations we fixed the magnetic moment per Fe ion and then scanned the total energy as a function of Fe-magnetic moment. Our results are summarized in Fig. 4. The zero of energy is taken as the M=0 case (i.e., NM calculation). From Fig. 4, it is clear that LaOFeAs has only one magnetic ground state which is AF2. The Ferro spin-configuration always results the highest energy regardless the Fe-magnetic moment. Similarly AF1 ordering always yields energies higher than the NM case. For the AF2 ordering, we see that the energy minimum occurs near the fixed moment calculation with M=1. Repeating calculations where magnetization is not fixed, we obtained the optimum magnetic moment as M=0.87 μ_B per Fe. As we discuss below in detail, the Fe magnetic moment is further reduced almost by a half when the structure is allowed to distort to due to AF2 stripe ordering.

One confusion with the DFT studies of Fe-pnictide is the calculated Fe-magnetic moment. The most of the calculations, in particular those based on pseudopotentials, give too large moment around 2.0 μ_B compared to experimental values of $0.3 - 0.8$ μ_B. In order to explain the small experimental moment, several theories based on quantum or thermal fluctuations have been proposed since the SDW system is magnetically frustrated[43]. On the other hand, there are studies suggesting that the small moment is due to electronic effects, local chemistry of Fe and its interaction with the As ions. It has been shown that a small displacement of As-z position and/or structural distortion can easily change the Fe-moment from 2.0 μ_B to 0.5 μ_B[21,34,35,44]. In section V, we will discuss this high sensitivity of the Fe-moment to the As-z position in detail in the context of giant magneto-elastic couping since z-position and c-axis of the crystal are coupled and have to be treated equally.

In order to gain a better insight into the nature of the magnetic interactions present in Fe-square lattice of the Fe-pnictide system, we map the calculated total energies of the F, AF1 and AF2 configurations shown in Fig. 4a to a simple Heisenberg like model $H = E_P + \sum_{i,j} J_{i,j} M_i M_j$ for a given fixed Fe moment M_i. For fully localized spin-systems this is a perfect thing to do but for the case of Fe-pnictide this is only an approximation. Nevertheless, the calculated Js should be a good indication of the magnetic interactions present in the system. We also note that these interactions are valid at high temperatures above the magnetic ordering transition where spin-flips are the relevant magnetic excitations (and not the spin-waves). Fig. 4b shows the *effective* J_1 and J_2 obtained from the energies of the F, AF1 and AF2 at given magnetic moment. The dependence of the Js on the magnetic moment further suggests that the simple Heisenberg Hamiltonian is not a good model for this system. Here we use the term *effective* because the calculated $J_{i,j}$ is actually the interaction between spins i and j plus the infinite sum of interactions between their periodic images. The calculations of magnetic interactions up to $4rd$-nearest neighbor will be discussed in the next section. From Fig. 4, it is clear that both J_1 and J_2 are quite large and positive (i.e., antiferromagnetic). J_2 is always larger than $J_1/2$ and therefore AF2 structure is the only ground state for any given moment of the Fe ion. By looking at the exchange paths for J_1 and J_2 (shown in insets to Fig. 4), we notice that the Fe-As-Fe angle is around 75° and 120° for nn and nnn Fe-pairs, respectively. Hence it makes sense that the 2nd nn exchange interaction is as strong as the nn exchange because the angle is closer to the optimum value of 180°.

We note that there are now a large number of studies of exchange interactions in Fe-pnictides based on vary different methods such as mapping energies to a Heisenberg model[21,32,45], linear response theories[34,46,47], strong coupling perturbation calculations of superexchange interactions within a tight binding model[48] and Kugel-Khomskii type effective Hamiltonian with spin and orbital degrees of freedom[49]. All these studies indicate that the major exchange interactions in Fe-pnictides are J_1 and J_2 that are large, comparable in magnitude and antiferromagnetic (i.e. frustrated). This seems to be the intrinsic property of FeAs plane that is common to all Fe-pnictide superconductors. It is quite surprising and also very interesting that there are strong and competing antiferromagnetic interactions in the Fe-pnictide system that result in a totally frustrated AF2 spin configuration. This is very similar to the magnetic ground state of the cuprates where the AF ordered 2D square lattices of the adjacent planes are frustrated[37]. Even though electron doping seems to destroy the long-range magnetic order, the short range spin fluctuations will be always present and probably play an important role in the superconducting phase, much like the high T_c cuprates.

Finally we note that there have been several neutron scattering measurements[14,50,51,52,53] of the spin-wave spectrum in 122 systems indicating $J_1 + 2J_2 \approx$

100 ± 20 meV. From Fig. 4, we get $J_1 + 2J_2 \approx 80$ meV for S=1 in 122 systems. Noting that our calculations were done much before the experimental measurements, the agreement is quite good and give confidence that DFT calculations actually work for predicting properties of Fe-pnictides. Similarly, based on our calculations[21], we had also predicted that orthorhombic lattice parameter along the parallel-aligned spin-direction should be shorter than the axis along the anti-parallel spin direction in the SDW phase, which has now been confirmed by experiments[14]. This further assures that all-electron DFT calculations capture many fine details of the physics in Fe-pnictides.

III. COMPETING MAGNETIC INTERACTIONS IN FE-PNICTIDES

In previous section we estimated some effective exchange interactions from the total energies of F, AF1, AF2 but from those estimates it is not clear if the calculated parameters are limited to the nearest neighbor interactions or not. If the exchange interactions originate from Fermi-surface nesting then they should be long range. If they originate from Fe-As-Fe superexchange then they should be short range. Hence by calculating $J_{i,j}(R)$ as a function of Fe-Fe distance R, we can determine if the Fermi surface nesting is the major factor in the magnetic exchange interactions and learn more about nature of these interactions and the way they couple to the lattice and the structural phase transition.

Here we address this issue by calculating exchange parameters from two different methods. We developed a systematic approach where the exchange parameter between spin-i and spin-j is obtained from the total energies of a reference magnetic configuration and those configurations obtained by flipping the spins i and j one at a time and simultaneous flipping both spins. From these four energies, it is possible to obtain the exchange constant between spin i and j. The details of this technique are presented in Appendix A. From now on, we refer to this method as "direct spin-flip method". Note that this method is more appropriate at very high temperatures where the relevant spin-excitations are spin-flipping rather than spin-waves.

The second method is based on linear response perturbation theory using Green function approach within rigid-spin-approximation[54,55,56] as implemented in openmx package[57]. Basically, we calculate the small energy change due to an infinitesimal rotation of spin i and spin j using Green function perturbation theory with the assumption that the magnitude of spins are fixed and only their orientations are changed. This is a questionable approximation for Fe-pnictides because the Fe-spin magnitude is very sensitive to the spin pattern as well as the As-position. In Sec. II, we have already seen that the spin-magnitude goes to zero if they are forced to be aligned ferromagnetically. With this in mind, we still think that when the system is at very low temperature where the spin-moment is fixed and spin-waves are valid, this perturbation approach should give physically correct results. Similar approach have been successfully used to study exchange interactions and spin-wave stiffness constants in transition metals such as bcc Fe[56].

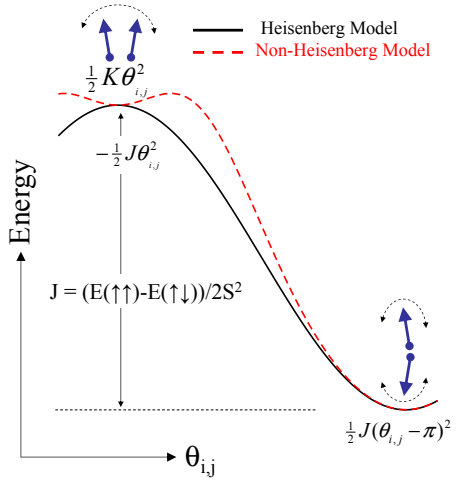

FIG. 5: (color online) Schematic representation of a spin-interaction energy versus the angle between spins i and j for a Heisenberg (black) and non-Heisenberg model (red). The linear response theory gives the second derivative of the energy at the local spin-configuration while the spin-flip method defines the exchange constant as the energy difference between parallel and antiparallel spin-configurations. For the Heisenberg model (black) both methods give the same energy, i.e. J. However for non-Heisenberg model, the linear response theory gives K (i.e. ferromagnetic for this example) while spin-flip method gives J (i.e. antiferromagnetic). Needless to say, both are correct! K describes the spin-dynamics near the bottom of the spin-interaction potential (i.e. spin-waves) while J describes the spin-dynamics near the energy barrier (i.e spins are flipping as in the paramagnetic phase).

It is very important to note that the calculated quantities from spin-flip and linear-response-theory are not the same thing and therefore these two methods can give totally different results for non-Heisenberg spin-interactions. This is schematically shown in Fig. 5. The linear response-theory gives the second derivative of the spin-interactions from infinitesimal rotation of the spins near their equilibrium positions. On the other hand, the spin-flip method gives the energy difference between parallel and antiparallel spin configurations. When we deal with Heisenberg interaction, $J(\theta)$ is proportional to $\cos(\theta)$ and therefore both the second derivative and the energy difference give the same answer. However for a non-Heisenberg model where the dependence of J on the angle is not a simple cosine as shown in Fig. 5, the linear response theory will give the 2nd derivative at the local structure, i.e. K in Fig. 5 while the spin-flip method will give J and therefore the two methods will differ. This should not be considered as one of the method is not working but rather as an evidence that the spin-spin interaction is not a traditional Heisenberg

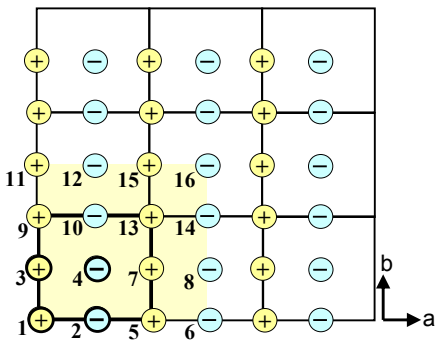

FIG. 6: (color online) The $3\sqrt{(}2)\times3\sqrt{(}2)\times1$ supercell considered in calculations of the exchange parameters in real-space. For simplicity, we show only the Fe ions with their number labels and spins (+ up, - down) according to AF2 ordering. The $J_{i,j}$ for each iron pairs i and j are plotted in Fig. 6. The shaded region indicates the half of the supercell in which we can extract the exchange interactions between any pairs of spins (which are numbered from 1 to 16 for convenience).

type. As we shall see below, this is indeed the case for Fe-pnictide where for the parallel-spin direction in the stripe phase, linear response theory will give a ferromagnetic interaction while the spin-flip method will give an antiferromagnetic interaction. Since the linear response theory probes the energy changes near the local-spin configurations due to small spin-rotations, the Js from this method should be used to explain the experimental spin-wave spectrum. However for spin-dynamics near or above the paramagnetic phase transition the spin-waves are not valid and therefore the Js from spin-flip method is more appropriate. Of course, since the Js depend on the spin-configurations considered one can not study the phase diagram of Fe-pnictides from zero to high temperatures with a single Heisenberg like Hamiltonian. In that case, it is important that one goes beyond the Heisenberg picture and consider more complete models such as Kugel-Khomskii Hamiltonian where the orbital and spin-degrees of freedom are treated self consistently on equal footing[49].

Finally, we note that both methods discussed above are based on periodic supercell approach and therefore what we calculate is actually the sum of the interactions between spin i and j and the interaction between their periodic images. Hence it is important to consider a very large supercell to make sure what we get is actually the individual exchange constant between spin i and spin j. Hence, we consider $3\sqrt{(}2) \times 3\sqrt{(}2) \times 1$ cell which has total 144 atoms, 36 of which are iron. Fig. 6 shows the labeling of the 32 iron atoms in the large supercell. The direct spin-flip calculations were done using the plane-wave code pwscf[42] with cutoff energy of 30 Ry and charge cutoff of 240 Ry using PBE-GGA exchange functional. We used 2x2x3 k-points. The perturbation calculations with rigid-spin-approximation were carried out using the package openmx[57] which implements numerical atomic arbitals and norm-conserving pseudopotentials. We used equivalent cutoff, k-point grid and the same PBE exchange functional as the pwscf calculations. We used experimental atomic positions for the LaOFeAs system without any structural relaxation. Both methods (i.e. pwscf and openmx) give an iron magnetic moment close to $\approx 2\mu_B$, a typical value obtained from pseudo-potential based methods. For convenience, in the discussion below, we report JS^2 by setting S=1 (rather than taking S=2 and recalculating Js).

Our results, for the exchange constants, $J_{i,j}(R)$ from both spin-flip and perturbation methods are shown in Fig. 7. We first discuss top panel in Fig. 7 which is from direct spin-flip method. The strongest interactions, i.e. $J_{1,2}, J_{1,3}$, and $J_{1,4}$ are all antiferromagnetic and comparable to each other, consistent with our previous results obtained from the total energies of three spin configurations discussed in section II. We note that the symmetry between a and b axis is broken and we obtain different J_1^a (i.e. $J_{1,2}$) and J_1^b (i.e. $J_{1,3}$). However the difference is small and they are both antiferromagnetic. The J_2/J_1 is around 1 (here J_2 is $J_{1,4}$) and therefore the AF2 (i.e. SDW) is the ground state. Fig. 7 also shows how the exchange constants decay with distance along the Fe-Fe square diagonal, and along a- and b-directions. We note that the anti-parallel-spin alignment is taken to be along the a-axis. Interestingly, $J_{i,j}(R)$ already changes sign and become ferromagnetic at the 2nd (i.e. $J_{1,5}$) and 3rd shells (i.e. $J_{1,10}$) along the $a-$ and b-axes, respectively. As shown in Fig. 7, along the $a-$ and $b-$directions, $J_{i,j}(R)$ has an oscillatory character with an envelop decaying as $1/R^3$. One exception to this decay rate is the $J_{1,4}$ (i.e. J_2), the exchange interaction along the Fe-Fe square diagonal direction. $J_{1,4}$ is very large (i.e. way above the $1/R^3$-envelop) and then basically goes to zero for further distances (i.e. $J_{1,13} = J_{1,16} \approx 0$). This suggest that the origin of $J_{1,4}$ is probably not the Fermi-surface nesting or other long-range exchange interactions but rather local superexchange interactions through As-p orbitals. In contrast, the nature of the exchange constants along the $a-$ and $b-$directions are very different. They are long range and decay with $1/R^3$, much like in bcc-Fe[56].

The bottom panel in Fig. 7 shows the calculated exchange parameters $J_{i,j}(R)$ obtained from linear response perturbation approach with rigid-spin approximation. Similar to results from spin-flip method, the exchange interaction along the Fe-Fe square is antiferromagnetic and very short range while along the $a-$ and b-directions it has oscillatory character with sign change and slow decay. The most important difference between the spin-flip and perturbation methods is the nearest-neighbor exchange interaction along the stripe direction, i.e. $J_{1,3}$. While spin-flip method gives this interactions as antiferromagnetic the linear response theory suggests it is weak but ferromagnetic. As discussed above and shown in Fig. 5, this difference between two methods is a nice evidence that the spin-interactions along the stripe direction is probably not a classical Heisenberg. In conclusion, due

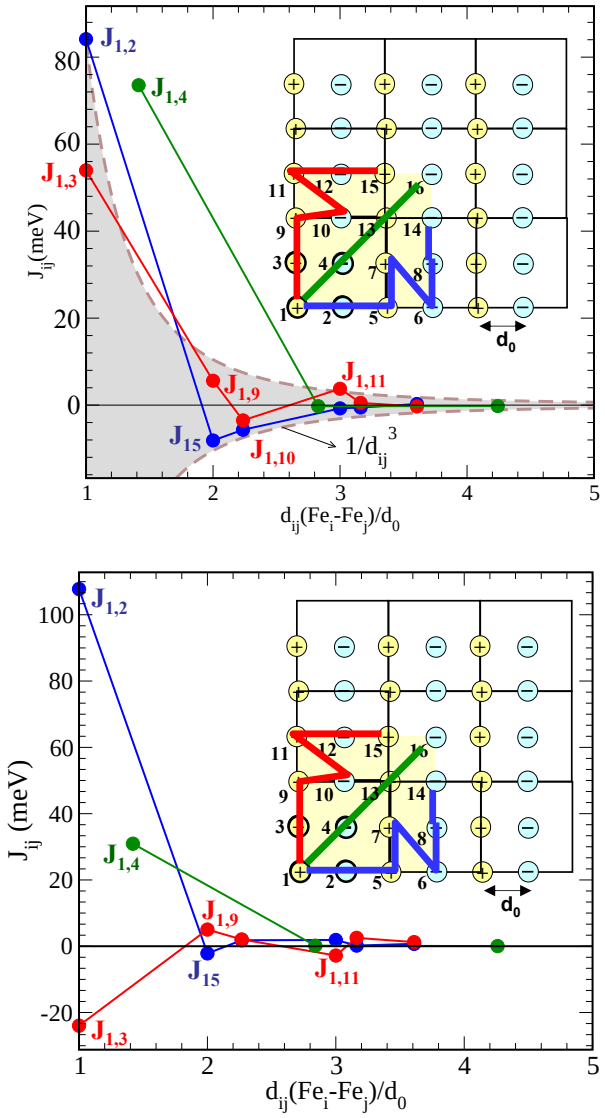

FIG. 7: (color online) The calculated exchange constants $J_{i,j}(R)$ (S in JS^2 is taken to be 1) along three different paths as shown in the inset. Top panel shows the results from direct spin-flip method while the bottom panel shows results from linear response perturbation method within rigid-spin-approximation. Both methods give strong and antiferromagnetic short range interaction along the diagonal direction while they differ for the parallel aligned spin-direction (i.e. b-axis). The dashed curves and the shaded area in top panel shows that the exchange interactions along the a and b axes are oscillatory with an envelop decaying as $1/R^3$, much like in the bcc-Fe[56].

to slow $1/R^3$ decay of Js along the stripe direction and its different sign obtained from spin-flip and linear response methods strongly suggest that the spin-interactions along the stripe direction is unusual, long-range and probably related to Fermi-surface nesting.

We note that our results from perturbation theory are in agreement with the earlier calculations reported from Pickett's group in Ref.46 where the spin-exchange constants were calculated in various 122 systems using linear response theory and small but ferromagnetic exchange interactions are found along the parallel-spin direction. We emphasize that since the exchange interaction along the stripe direction (i.e b-axis) is ferromagnetic, the frustration is totally removed and there is nothing special for the ratio $J_1^a/2J_2$ being ≈ 1 anymore. Finally, we note that there is an other interesting report by Balashchenko and Antropov[47] where the exchange interactions are calculated in real space as a function of As z-position using linear response theory. As expected, they observe magnetization changes from $1.3\mu_B$ to $0.31\mu_B$ with a small displacement of arsenic z-position which in turn changes the Fe-As bond distance by about 0.1 Å. However the calculated exchange parameters do not agree with those reported from Pickett's group even though both groups use linear response theory. They found that all the major interactions are antiferromagnetic with significant anisotropy along the parallel and antiparrallel spin directions. This anisotropy is found to be very sensitive to the As z position. However for all z-positions studied, the exchange along the stripe direction is always antiferromagnetic. The authors also conclude that the interactions are long range in agreement with our results for the spin directions along the $a-$ and $b-$axis. However we emphasize that from both methods used here, we find that the diagonal spin interaction (i.e. J_2) is very strong and antiferromagnetic for only the nearest neighbor and then basically becomes zero for further distances.

Since two methods shown in Fig. 7 give opposite spin-interactions along the stripe direction (i.e. parallel spin-direction), an interesting picture emerges from these two calculations. At high temperature where the system is paramagnetic or close to magnetic ordering , we find that the major magnetic interactions are antiferromagnetic and frustrated. The exchange interactions along a- and b-directions are comparable to each other as it should be due to tetragonal symmetry of the paramagnetic state. As the system orders and the spin-flip excitations become more and more spin-oscillations as in the case of spin-waves, the band structure is modified (i.e. the symmetry between d_{xz} and d_{yz} is broken) yielding very different exchange interactions along a- and b-directions. In the low-temperature limit where the spins are pretty much fixed, we expect the perturbation results valid and should replace the spin-flip results.

Due to non-Heisenberg nature of the spin-interactions that we obtain here, one has to be careful in modeling these systems using a Heisenberg like model. For a given spin-configuration, it is probably OK to use a Heisenberg model to study low-energy excitations in that configuration (such as spin-waves in SDW ordered state). However if one wants to study the whole phase diagram as a function of temperature, a simple Heisenberg model with a fixed Js is clearly not appropriate. As the spins rotate or change configurations, one will obtain totally different exchange constants. Hence in this case, one needs to go beyond the classical Heisenberg model to treat the Fe

$d-$orbitals and spin degrees of freedom on equal footing. Hence a Kugel-Khomskii like Hamiltonian could be more appropriate for Fe-pnictide systems. Recently a complicated phase diagram of spin-orbital ordering of Fe-pnictide has been studied in Ref.49 and we refer the reader to this study for details.

We finish this section with a brief discussion of the experimental determination of the exchange parameters in Fe-pnictides from inelastic neutron scattering experiments. Even though, Heisenberg model is not appropriate as discussed above, it is probably good enough to describe the spin-wave excitations at low temperatures where the spins are not flipping and therefore the exchange constants are not changing. A minimal spin Hamiltonian for Fe-pnictide may be written as

$$\mathcal{H} = \frac{1}{2}\sum_i \sum_{\alpha=a,b,d,c} J_\alpha \vec{S}_i \cdot \vec{S}_{i,\delta_\alpha} - D\sum_i S_{ix}^2 \qquad (1)$$

where the i-summation runs over all Fe-spins and J_α ($\alpha = a, b, c, d$) are the exchange interactions along the antiparallel spin direction a, along the parallel spin-direction b, along the c-axis, and finally along the Fe-Fe square diagonal, respectively. The last term is the easy-axis single ion anisotropy which originates from spin-orbit coupling. Usually it is small but here due to very large J_a and J_d, it is important to keep this term which can give large spin-gap at gamma that is proportional to $\sqrt{D \times (J_a + 2J_d)}$. The spin-wave spectrum of this Hamiltonian can be easily obtained by considering the AF2-spin configuration as helimagnetic ordering with modulation wavevector $Q = (\pi, 0, \pi)$ such that the spins are ordered antiferromagnetically along the $a-$ and $c-$ axis and ferromagnetically along the b-axis. We note that the unit cell of the helimagnetic spin-structure is twice smaller than the chemical cell along all directions (i.e. $a_M = a_o/2, b_M = b_o/2$, and $c_M = c_o/2$). Within this helimagnetic description of the cell, the above model Hamiltonian has a single spin-wave mode

$$\begin{aligned} \omega(\mathbf{q}) &= 2S\sqrt{A_\mathbf{q}^2 - B_\mathbf{q}^2} \\ A_\mathbf{q} &= J_a - J_b[1-\cos(q_b)] + 2J_d + J_c + D \\ B_\mathbf{q} &= J_a\cos(q_a) + 2J_d\cos(q_a)\cos(q_y) + J_c\cos(q_c) \end{aligned} \qquad (2)$$

and the zero-temperature inelastic structure factor (which is proportional to inelastic neutron scattering intensity)

$$S(\mathbf{q},\omega) = \sqrt{\frac{A_q - B_q}{A_q + B_q}}\delta(\omega - \omega_q) \qquad (3)$$

After having determined the eigen-spectrum of our model Hamiltonian, we now discuss how one may measure them using inelastic neutron scatting. Because of the tetragonal symmetry of the paramagnetic phase, during the SDW transition the single crystal samples will probably have orthorhombic twinning which we call ab-domains. In one domain the stripe direction (i.e. parallel aligned spin direction) will be along the a-axis while in the other domain it will be along the b-axis. In other words, even though we have a single crystal sample, we can not distinguish the wave-vector $\mathbf{q} = (q_a, q_b, q_c)$ from $\mathbf{q} = (q_b, q_a, q_c)$. Hence, from inelastic neutron scatting one will therefore probe the superposition of the spin-wave modes at these two wave-vectors, i.e. $\omega(q_a, q_b, q_c) + \omega(q_b, q_a, q_c)$. As we shall see below, due to very different ordering of spins along the $a-$ and $b-$ axes, the superposition of these two modes can be, in principle, resolved at high energies and in particular at zone-boundaries.

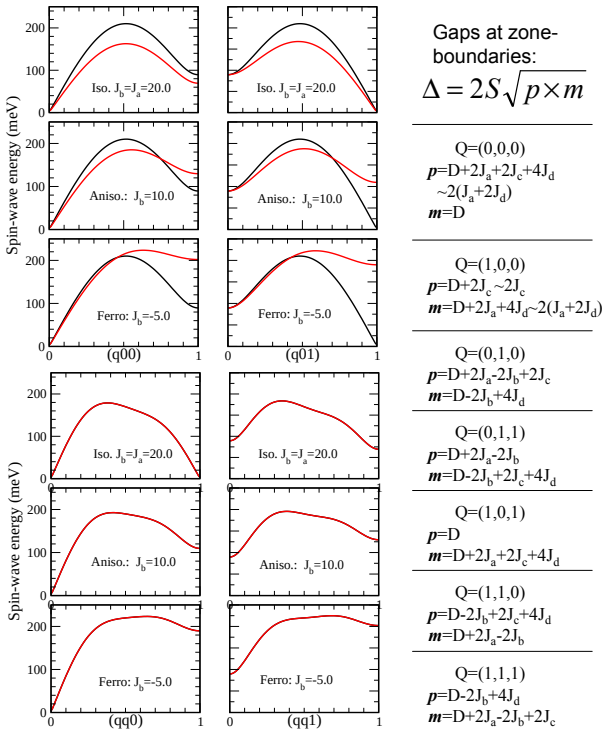

FIG. 8: (color online) The $ab-$domain-averaged spin-wave spectrum along (q,0,h) and (q,q,h) directions (h=0, 1). The black and gray (red) curves are due to spin-waves coming from domain-a and domain-b where the stripe direction is along the a- and b-axis, respectively. Note that with a proper constant momentum and/or energy scans, it should be possible to resolve two modes from two domains and uniquely determine the sign of exchange parameter J_b. On the right, we give the analytical expressions for the spin-wave gaps at different Brillouin zone boundaries. The plots are obtained using the following values (all in meV); $J_d = 40.0, J_a = 20, J_c = 5.0, D = 0.015$.

In Fig. 8 we show the $ab-$domain averaged spin-wave spectrum, i.e. $\omega(q_a, q_b, q_c)+\omega(q_b, q_a, q_c)$, along various directions. For the exchange parameters, we consider three cases; isotropic model ($J_a = J_b$), anisotropic model (i.e. $J_b = J_a/2$), and finally ferromagnetic model ($J_b < 0$). The values of the exchange parameters used in the calculations are given in Fig. 8. From Fig. 8, it is clear that contributions due to $a-$domain (red-curve) and $b-$domain (black curve) are quite different and could be

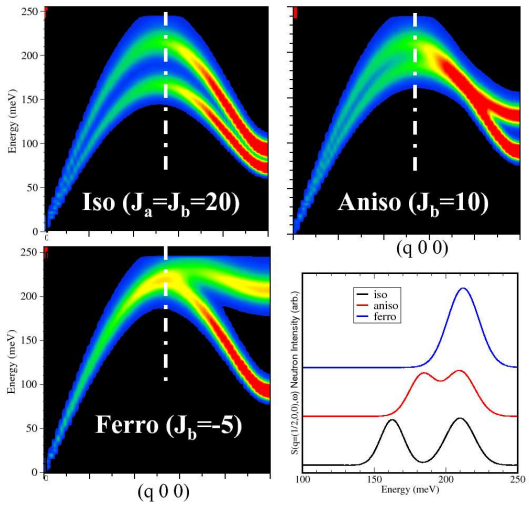

FIG. 9: (color online) The contour plot of calculated $S(\mathbf{q},\omega)$ for iso, aniso, and ferro-model for J_b along (q,0,0)-direction. The energy scans at constant q=(1/2,0,0) for the three models are indicated by dashed-line and shown in the bottom right panel. Note that despite the presence of orthorhombic-twinning, the spin-wave spectrum of the three models are quite distinct suggesting that one may uniquely determine the sign of J_b. All these are based on the assumption that the Stoner-continuum will not over-damp the spin-wave spectrum.

resolved experimentally. Interestingly for the isotropic model ($J_a = J_b$), the spin-wave spectrum is the most anisotropic near the zone-center and near the middle of the $(1/2, 0, 0)$ as shown in Fig. 8. This is due to the fact that the spins are aligned antiparallel and parallel along a and b axes, respectively while their interactions are forced to be equal and antiferromagnetic. This gives very different dispersion along the a- and $b-$axis and therefore one can resolve the two peaks in the $ab-$domain averaged spectrum. From Fig. 8, it is clear that near the $(1, 0, 0)$, the isotropic model have two modes near zero energy while the anisotropic and ferromagnetic models have one mode that has a huge spin-wave gap that is proportional to $\sqrt{(J_a - J_b)(2J_d - J_b)}$. The analytical expressions for the spin gaps at various Brillouin zone boundaries are given in Fig. 8. Finally, we note that $(qq0)$ direction is a special one where we should see only a single mode which has a tiny gap at (100) if the interactions are isotropic and a gap about the half of the maximum spin-wave energy for the anisotropic model. For the ferromagnetic model, the gap is almost the same as the maximum spin-wave energy (see left bottom panel in Fig. 8).

In Fig. 9, we show the $ab-$domain averaged inelastic-structure factor to get an idea about the intensities of the modes from two domains. The calculated spectrum is convoluted with Gaussian and 5% energy resolution. Fortunately the intensities from both domains are comparable and therefore it should be feasible to detect these modes in a multi-domain sample. As an example, in Fig. 9, we show energy scans at constant wavevector $Q = (1/2, 0, 0)$ for the three modes, which show very distinct spectrum for each model.

As a final note, we point out that in practice, the observation of spin-waves in Fe-pnictide could be problematic at high energies due to strong spin-wave damping by Stoner-continuum. However very recent inelastic neutron scattering measurements on Ca122 system[53] has revealed steeply dispersive and well-defined spin waves up to an energy of $\approx$ 100 meV. Unfortunately the resolution and the quality of these recent data are not good enough to carry out a detailed analysis as discussed here in order to determine the sign of J_1^b. We hope that in the near future there will be more experimental data with better resolution and quality.

IV. STRUCTURAL PHASE TRANSITION IN FE-PNICTIDES

We next discuss the implication of the magnetically frustrated AF2 configuration on the structural distortion which is shown to be a common feature of 1111 and 112 parent compounds[14]. Experimentally it has been demonstrated that magnetic SDW ordering and the tetragonal-orthorhombic distortion are closely coupled[58]. Interestingly for 1111 systems (i.e. LaOFeAs)[15] , the tetragonal distortion first takes place about 20-30 K higher in temperature than the magnetic transition. The transition for 1111 system is somewhat weak. On the other hand, for the 122 systems (such as $BaFe_2As_2$), it is clear that both transitions occur at the same time. They are more or less strong first-order type and one study suggests that the structural distortion is proportional to the magnetic order parameter (rather than its square)[58].

In order to establish a connection between the structural distortion and the magnetic ordering, we calculate the total energy as a function of the γ angle as shown in the inset to Fig. 10 for NM, F, AF1, and AF2 spin configurations (see Fig.3). When $\gamma = 90^o$, we have the original tetragonal cell. Once the γ deviates from 90^o, the original $\sqrt{2} \times \sqrt{2}$ structure (shown as dashed line) is no longer tetragonal but orthorhombic (i.e., the cell length along a and b axes are no longer equal). We note that for $\gamma = 90^o$, the orbitals d_{xz} and d_{yz} are degenerate and therefore one may think that the system is subject to symmetry lowering for reasons similar to those in a Jahn-Teller distortion. However as shown in Fig. 10, we do not see any distortion for any of the NM, F, and AF configurations.

The total energy versus γ plot shown in Fig. 10 clearly indicates that only AF2 ordering distort the structure with $\gamma = 91.0^o$, which is in good agreement with the experimental value of 90.3^o. The FP-LAPW method with LDA approximation we get M=0.48 μ_B which is in excellent agreement with the experimental value of 0.35 μ_B. Hence all electron-calculation is able to reproduce both the observed structural distortion and the small Fe-moment simultaneously. On the other hand, PW calcu-

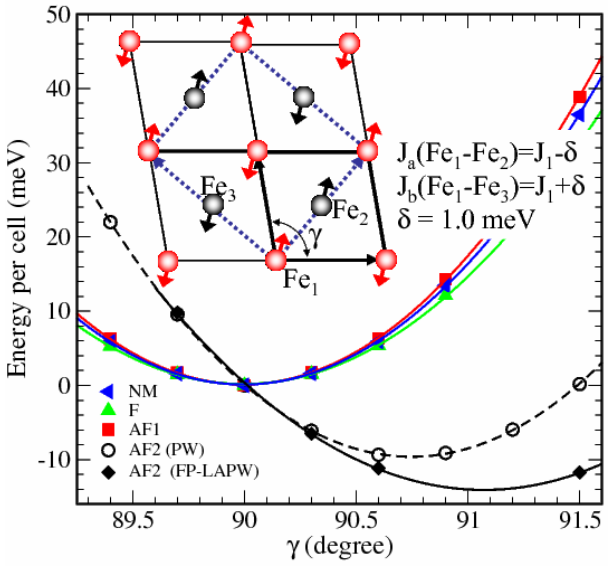

FIG. 10: (color online) The total energy per cell versus the angle γ for non-magnetic (NM), Ferromagnetic (F) and two antiferromagnetic (AF1 and AF2) spin-configurations. Note that only the AF2 spin configuration yields structural distortion. The inset shows that as γ increases, the ferromagnetic aligned Fe ions (i.e., Fe_1-Fe_2) get closer while the antiferromagnetically aligned ions (i.e., Fe_1-Fe_3) move apart, breaking the four-fold symmetry and thus the degeneracy of the d_{xz} and d_{yz} orbitals. For the AF2, the solid and dashed lines are from pseudo potential plane wave (PW) and FP-LAPW calculations, respectively.

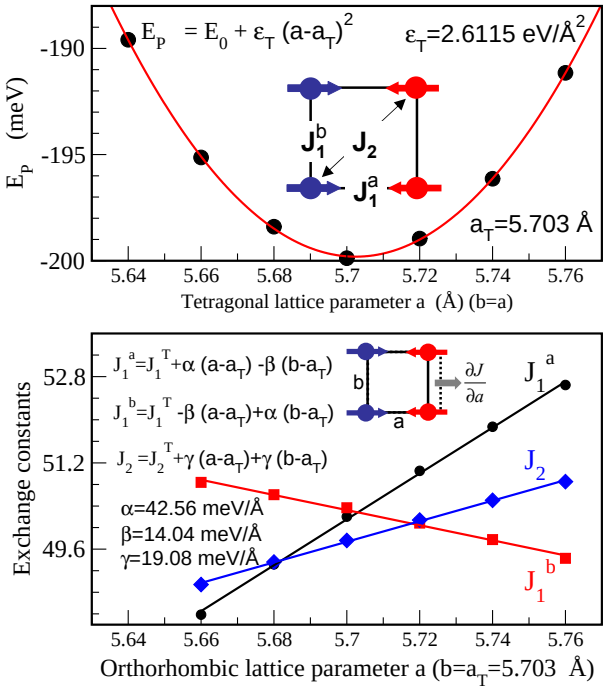

FIG. 11: (color online) Top: The paramagnetic portion of total energy (E_P) versus the tetragonal lattice parameter a (a and b are taken to be equal). The inset shows the SDW ordering, the relevant exchange constants and the fit to the total energy. Bottom: The linear expansion of the exchange constants with respect to lattice deformation. The tetragonal cell is distorted along a-direction while the b-axis is kept constant at $b = a_T = 5.703$ Å. Points are the actual calculations and solid lines are the linear fit.

lations with GGA approximation (dotted line) give good structural parameters when spin-polarization is allowed but then the calculated moment is too large. Somehow the magnetic ground state is over-stabilized in PW calculations. Therefore one has to be careful in studying the magneto-elastic couplings by PW methods, which will be underestimated. The net energy gain by the structural distortion shown in Fig 10 is about 12 meV per cell, which is of the same order as the temperature at which this phase transition occurs. We also considered two types of AF2 where the spins along the short axis are aligned parallel or anti-parallel (see Fig. 3c-d). These two configuration are no longer equivalent. According to our calculations the configuration in which the spins are ordered parallel along the short-axis is the ground state. This prediction[21] has now been confirmed by neutron scattering measurements for several 122 systems[14], giving us confidence that first-principles calculations describe many fine details of Fe-pnictide systems accurately.

Even though full structural optimization discussed above clearly shows that AF2 ordering gives rise to observed orthorhombic distortion with the long axis along the anti-parallel spin direction, it is not obvious why this happens. Naively one would expect the opposite, i.e. parallel spin-direction is the frustrated one and therefore it should get longer to decrease the antiferromagnetic interactions. This would be the case if we had Cu-O-Cu linear bond. However in the Fe-pnictide case, the arsenic ions are not directly between two Fe-ions (see Fig. 2) but they are above/below the Fe-squares. Hence when Fe-Fe distance is increased along a-axis, the Fe-As-Fe bond angle also increase along this direction while Fe-As distance does not change at first order. In fact, As ions are pulled down to keep the rigid FeAs bond fix and increase the angle. However the net effect of the increase in angle on the exchange interaction itself is not easy to predict due to complicated nature of the problem.

To determine if the exchange interaction J_1^a increases while J_1^b decreases during the orthorhombic transition, we calculate the lattice dependence of the exchange parameters, i.e. dJ/da, and then develop a simple spin-Peierles like model which successfully explains both the transition and the lattice parameters of F, AF1 and AF2 spin configurations within a unified picture.

In order to obtain the lattice-parameter dependence of the Js, we calculate the energies of F, AF1 and AF2 configurations for different tetragonal lattice parameters and then extract the E_P, the paramagnetic portion of the total energy as a function of tetragonal cell a. This is shown in the top-panel of Fig. 11. The tetragonal elastic con-

stant is then extracted by fitting the total energy to a quadratic form as shown in the figure. After having determined the paramagnetic contribution of the total energy, we then apply tetragonal to orthorhombic distortion by varying the lattice parameter along a-direction. For each distortion, we then calculate the energies of F, AF1 and AF2 spin-configurations. For each spin-configuration the internal atomic coordinates such as As z-position are always optimized. Using the energy expressions given in Fig. 3, we then extract the J_1 and J_2 which are given in the bottom panel of Fig. 11. We note that J_1^a increases and J_1^b decreases linearly as the a-axis is elongated. Similarly, the J_2 always increase with increasing lattice parameters near the paramagnetic optimum tetragonal cell parameter a_T as shown in Fig. 11. Hence it seems that both J_1 and J_2 increases with increasing bond-angle.

Now, using the lattice parameters dependence of J_1^a, J_1^b, and J_2 calculated in Fig. 11, one can easily obtain the new lattice parameters of the magnetic cell for ferro, AF1 and AF2 spin configurations which are summarized below:

$$F \rightarrow a = b = a_T - (\frac{2\delta}{\epsilon_0} + \frac{\alpha - \beta}{\epsilon_0}) < S^2 > = 5.677\mathring{A}\ (5.625\mathring{A}) \quad (4)$$

$$AF1 \rightarrow a = b = a_T - (\frac{2\delta}{\epsilon_0} - \frac{\alpha - \beta}{\epsilon_0}) < S^2 > = 5.699\mathring{A}\ (5.701\mathring{A}) \quad (5)$$

$$AF2 \rightarrow a = a_T + (\frac{2\delta}{\epsilon_0} + \frac{\alpha + \beta}{\epsilon_0}) < S^2 > = 5.739\mathring{A}\ (5.734\mathring{A}) \quad (6)$$

$$b = a_T + (\frac{2\delta}{\epsilon_0} - \frac{\alpha + \beta}{\epsilon_0}) < S^2 > = 5.696\mathring{A}\ (5.668\mathring{A}) \quad (7)$$

Here the numbers given in parentheses are the results from self consistent full cell relaxation calculations. From above results, it is clear that this simple model explains most of the observed features such as F and AF1 ordering does not distort the lattice. Ferro magnetic cell has the smallest lattice parameter because the system wants to make both J_1 and J_2 smaller as they are antiferromagnetic and we are forcing the spins ferromagnetically ordered. Similarly, for AF1 ordering, we get competitions between J_1 which wants to increase the lattice while the J_2 term is still not satisfied and therefore it wants the lattice shrinks, yielding a lattice parameter larger than ferro but smaller than AF2. In the case of AF2, the J_2 is totally happy and want to increase the lattice. Our model for AF2 nicely predicts orthorhombic distortion with right lattice parameters.

Finally we note that all of our discussion given above is basically based on a single FeAs layer without inter-plane interactions. In reality these systems order three dimensionally at the structural phase transition. This raises a questions; is there any correlation between the

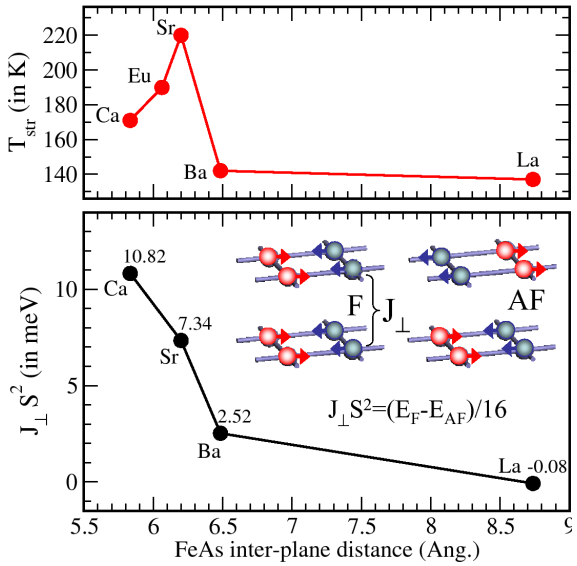

FIG. 12: (color online) Top: The structural phase transition temperature T_{str} versus FeAs interplane distance for M122 (M=Ca, Eu, Sr, and Ba) and La1111 systems. Bottom: The calculated interplane exchange interactions $J_\perp$ (in meV) versus FeAs interplane distance. For the La1111 system, the energy difference between AF and F magnetic configurations (shown in the inset) is too small to get an accurate number but it is less than 0.2 meV. Experimentally[14] $J_\perp$ in 1111 systems is also found to be very weak with both positive and negative sign depending on the rare-earth in the system. The inset shows the ferro and antiferro alignments of the FeAs planes in the unit cell. Here E_F and E_{AF} are the total energies per cell (i.e. 8 Fe atoms). Note that while $J_\perp$ drops sharply with increasing Fe-Fe interplane distance, T_{str} first increases and then drops with increasing Fe-Fe distance.

structural phase transition T_{str} and the inter-plane magnetic interaction $J_\perp$ between FeAs planes. Normally the larger the $J_\perp$ the higher the T_{str} should be. To answer this question, we have calculated $J_\perp$ for different 122 systems and plot it as a function of Fe-Fe plane distance in Fig. 12. From this figure it is clear that structural phase transition temperature T_{str} does not have a monotone dependence on Fe-Fe distance while $J_\perp$ does. This suggest that there must be an other factor which effects the T_{str} in an opposite way. One possibility could be the shear modulus of the system. If the c-axis is short, then the chemical bonding between FeAs planes would be stronger making the structural distortion difficult. On the other hand, the smaller c-axis means the larger $J_\perp$ which means larger in-plane AF2 correlation that drives the structural phase transition. Since the effects of shear-modulus and $J_\perp$ are opposite, T_{str} could have a maximum at a particular FeAs interplane distance as indicated by the experimental data. Currently we are developing a phenomenological Landau-theory along these lines to address the remaining issues discussed above and our results will be published elsewhere[59]. We note that there have been already a large number of theories[60,61,62,63] to describe this

coupled structural and magnetic phase transitions. We refer the reader to these studies for details[60,61,62,63].

V. GIANT MAGNETO-ELASTIC COUPLING IN FE-PNICTIDES

In order to get a general understanding giant magneto-elastic coupling present in iron-pnictides, here we consider one example of each class of pnictides; namely $CaFe_2As_2$ for the 122 system with the smallest Ca-ion available and the BaFe2As2 with the largest metal Ba. For the 1111 system, we consider LaOFeAs. We also study a doped 122-system, i.e. $Na_{0.5}Ca_{0.5}Fe_2As_2$. Since in our $\sqrt{2} \times \sqrt{2}$-cell we have four chemical formula, we consider a supercell where two Na and two Ca are ordered. For each given system, we have performed full structural optimization including the lattice parameters and the atomic positions. We consider our optimization is converged when the maximum force on each atom is less than 0.005 eV/Å and the pressure is less than 0.1 kbar. We have performed the full structural optimization for non-magnetic (NM), i.e. "non-spin polarized", checkerboard antiferromagnetic (AF1) and stripe (AF2) spin configurations. Our results are summarized in Table 1. As expected, the ground state for all four systems is the stripe AF2 phase and the optimized parameters are in good agreement with the experimental data at ambient conditions.

The most striking and surprising finding listed in Table 1 is the giant dependence of the optimized c-lattice parameter on the spin-configuration considered. For the case of $CaFe_2As_2$, we note that AF1 configuration is the next stable state (after the AF2) but the c-value is significantly reduced; 11.63 Å versus 10.60 Å for AF2 and AF1 spin configurations, respectively. This difference in c is not due to different AF1 and AF2 spin configuration but due to different Fe-spin state in AF1 and in AF2. The difference is even larger, when the Fe-magnetism is totally ignored (i.e. non-spin polarized calculations). The optimized z-value for NM-state is 10.39 Å, which is 1.34 Å shorter than the experimental value at ambient pressure. We note that the optimized lattice parameters, a=5.65 Å and c=10.39Å for the NM phase are in reasonable agreement with the neutron data in the collapse phase (a=5.8 Å and c=10.6 Å)[64]. Hence from these results and the recent experimental observation of the collapse-T phase, one can reach the conclusion that the Fe-moment should be present in 122 systems at all times at ambient pressure. This is because we know that these systems are ordered in an AF2 spin configuration when they are not doped or superconducting. When they are doped and superconducting we do not see huge changes in their c-lattice parameters. This indicates that even though the AF2 long range ordering is destroyed with doping or we are at temperatures above the magnetic ordering transition T_N, the Fe-spin should be present in the system. Otherwise, we should see the expected huge reduction in the c-axis. In other words, the iron-pnictide system should be considered as paramagnetic i.e. with the on-site non-zero iron moment without any long range order. We note that the paramagnetism is different than the "non-magnetic" case that we consider in our DFT calculations where we force equal up and down spins in each orbital. The non-spin polarized calculations should not be considered as a model for the paramagnetic system. With the standard density functional theory, there is no way to treat a paramagnetic system (i.e. we have the spin-degrees of freedom at each site but no long range order).

TABLE I: Various optimized structural parameters for NM, AF2, and AF1 spin configurations, respectively. Note that the c-axis from non-spin polarized and AF1-spin configurations are significantly smaller than the experimental data at ambient conditions. The zero of energy is taken as the energy of the NM-case. The experimental data are taken from Refs[7,9,15,22]. *The AF1 configuration goes to NM during structural optimization for $Ca_{0.5}Na_{0.5}Fe_2As_2$.

	a	b	c	As(z)	d_{FeAs}	M_{Fe}	E (meV)
$CaFe2As_2$							
NM	5.63	5.63	**10.39**	0.36251	2.309	0	0.0
AF1	5.65	5.65	**10.60**	0.36440	2.338	1.3	-16
AF2	5.61	5.48	11.61	0.36695	2.367	2.2	-100
Exp.	5.68	5.68	**11.73**	0.3665	2.370	1.0	–
$Ca_{0.5}Na_{0.5}Fe_2As_2$							
NM	5.59	5.59	10.52	0.36284	2.31	0	0.0
AF1*	5.59	5.59	10.52	0.36284	2.31	0	0.0
AF2	5.43	5.53	12.05	0.36536	2.382	2.4	-97
Exp.	5.42	5.42	11.86	–	–	0.0	–
$BaFe2As_2$							
NM	5.58	5.58	12.45	0.3479	2.319	0	0.0
AF1	5.64	5.64	12.73	0.35231	2.382	2.1	-80
AF2	5.70	5.59	12.83	0.3549	2.408	2.4	-169
Exp.	5.52	5.52	13.02	0.3545	2.397	1.0	–
LaOFeAs							
NM	5.64	5.64	8.59	0.35944	2.332	0	0.0
AF1	5.69	5.69	8.71	0.35128	2.393	2.1	-86
AF2	5.67	5.73	8.72	0.34860	2.409	2.4	-190
Exp.	5.70	5.70	8.737	0.3479	2.407	0.35	–

Fig. 13 shows an energy reaction path without any energy barrier for the collapse of $CaFe_2As_2$ with the lost of Fe-spin. It is surprising that the c-lattice parameter reduces from 11.7 Å to 10.4 Å but yet the total energy change is only 0.3 eV per cell (i.e. four Fe ions). One wonders how the atoms are rearranged during the collapse of c-axis. Do the FeAs planes remain rigid and get close to each other? Does this collapse have anything to do with the effective radius of Fe-ion for different Fe-spin states? Our answer to these questions is simply no. First of all, the collapse of the c-axis happens rather uniformly. There is significant and comparable decrease in the height of the Fe-As and As-Ca-As planes, indicating that the whole lattice almost uniformly shrinks. In our earlier study[65] we traced down the origin of this huge c-

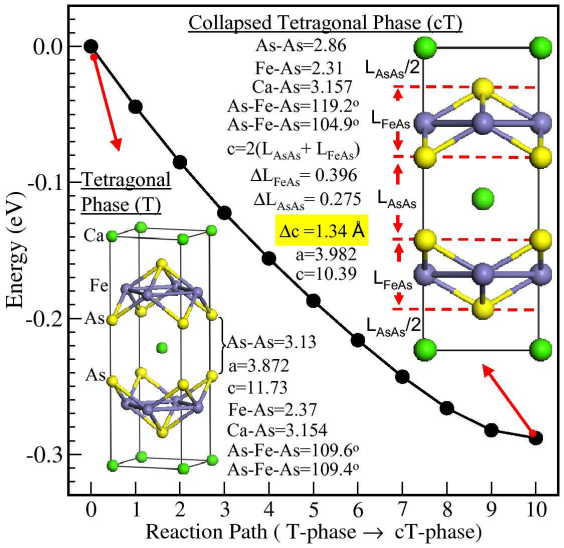

FIG. 13: (color online) Total energy along a reaction path, showing that the Ca122 tetragonal phase goes to collapsed-tetragonal phase without any energy barrier during non-spin polarized structural optimization. The energy gain due to 1.34 Å c-axis collapse is about 0.3 eV. The insets show the initial (T-Phase) and final (cT-phase) Ca122 structures with relevant bond-distances (in Å) and angles (in degrees). Note that in the cT-phase the change in the height of the FeAs (ΔL_{FeAs}) and the As-Ca-As (ΔL_{AsAs})planes are comparable, indicating a uniform compression of the whole lattice.

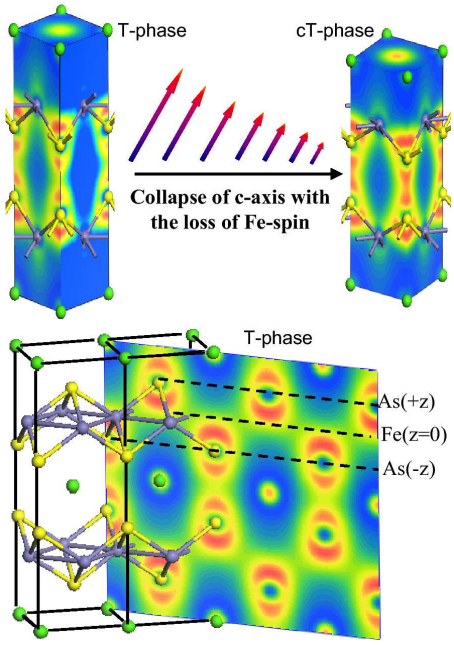

FIG. 14: (color online) Contour plot of one of the orbitals which is responsible for the discovered As-As covalent bonding for T-phase (top-left) and cT-phase (top-right), respectively. Note that the As-As bonding present in both phases is much more significant in the cT-phase. The bottom panel shows an other orbital on a slice along (110) plane, indicating clear hybridization between intra-As atoms below and above the Fe-plane in the T-phase.

axis collapse to large As-As interaction between adjacent FeAs planes.

In order to demonstrate that there are large hybridization between As ions in the Ca122 system, we show the contour plots of the relevant orbitals in Fig. 14. Again the contour plots in the T- and cT-phases are quite similar. It is very clear that the As ion below the top Fe-plane makes a bond (or hybridizes) with the arsenic ion which is above the lower Fe-plane. Hence this overlap of the As-As along the c-axis makes this system quite isotropic and far from being layered system. From Fig. 14 it is clear that the As-As bonding along the c-axis got significantly stronger. According to bond-population analysis, the bond strength increased almost twice. Due to close proximity of the As ions in adjacent Fe-layers, the observation of the As-As interaction is probably not that surprising. What is surprising is to see that there is almost the same type of hybridization between two arsenic ions on the same Fe-plane as shown in the bottom panel of Fig. 14.

Since we have shown that the As ion above the Fe-plane has a strong overlap with the As ion below the same iron plane, their interaction is automatically increased as the Fe-As interaction decreases due to decrease in the Fe-moment which changes the chemistry of the Fe ion. Therefore, we have now a mechanism which explains why the As ion z-values get shorter with the decreasing Fe-moment. Our mechanism also explains why we see a smaller reduction in the c-axis for the LaOFeAs than the 122 system as listed in Table 1. The reduction in the c-axis in the LaOFeAs system is due to the intra-plane As-As interaction only since there are no two adjacent FeAs planes to interact with each other as in the case of Ca122. Our theory also predicts that for larger ions like Ba, we should see less c-reduction because the As-As distance between two adjacent planes are now larger due to larger ionic radius of Ba. In Table 1, we also show that similar c-reduction with Fe-spin occurs in the doped $Na_{0.5}Ca_{0.5}Fe_2As_2$ system as well.

Since our results suggest that Fe-magnetism is totally lost in the cT-phase, one wonders if the $\sim$ 12 K superconductivity observed in some experiments in the vicinity of the collapse cT-phase of $CaFe_2As_2$[66] can be explained by conventional electron-phonon (e-ph) coupling? In order to address this question, we have calculated phonon spectrum and Eliashberg function from linear response theory[42]. We used basically the same method and the equivalent parameters that are used in Ref.67 for LaOFeAs. Our results are summarized in Fig. 15 and very similar to those for LaOFeAs. We obtained a value of electron-phonon coupling $\lambda = 0.23$ and the logarithmically average frequency $\omega_{log} = 218$ K, which gives $T_c = 0.6$ K using the Allen-Dynes formula with $\mu^* = 0$ (i.e. an upper bound for T_c). Hence, if the $\sim$ 12 K superconductivity observed in some experiments

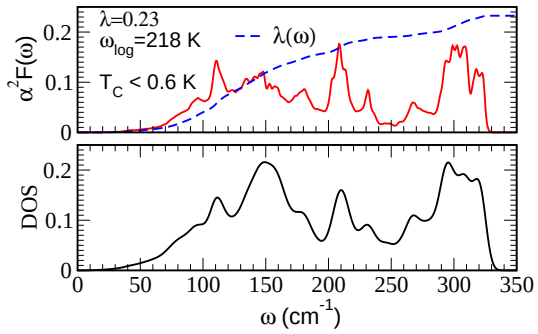

FIG. 15: (color online) Phonon density of states (DOS), Eliashberg function ($\alpha^2F(\omega)$) and the frequency-dependent e-ph coupling $\lambda(\omega)$ (dashed line) for $CaFe_2As_2$ in the cT-phase.

can be confirmed to be actual bulk superconductivity in the cT-phase, it would mean that the mechanism of superconductivity in the cT-phase of $CaFe_2As_2$ is likely unconventional and it has nothing to do with Fe-magnetism which is not present in the cT-phase. On the other hand, if the future experiments totally rule out that the cT-phase of Fe_2As_2 does not show bulk superconductivity then it would mean that the Fe-magnetism is required for the superconductivity in these systems. Because of these reasons, the cT and T-phases of $CaFe_2As_2$ provide us an invaluable opportunity to study the same system with and without Fe-magnetism. We hope that there will be more focus on the superconducting properties of $CaFe_2As_2$ system under pressure to resolve the outstanding issues about the $\sim$ 12 K superconductivity observed in some experiments.

In conclusion, we have revealed surprisingly strong As-As interactions for both intra- and inter-plane arsenic ions. The strength of this interaction is controlled by the Fe-As chemical bonding. Reducing the Fe-moment, reduces the Fe-As bonding, which in turn increases the As-As interaction along the z-axis, causing arsenic atoms on opposite sides of Fe-square lattice to move towards each other. This explains the high sensitivity of the z-atom positions and the large reduction of the c-axis with the Fe-magnetic moment. From visualization of the electronic orbitals, we show that the 122 systems should not be considered as layered systems since the As-As inter-plane interaction is as strong as the intra-plane As-As interaction. The 122 system are in fact quite 3D isotropic than one initially thinks. Since at ambient pressure, we do not observe large c-axis drops in the superconducting samples, we conclude that the Fe-magnetic moment should be present at all times in these systems, at least in 122 materials such as $CaFe_2As_2$. In other words, the iron-pnictide system should be considered as paramagnetic (i.e. Fe-moment is present without long range order). Non-magnetic treatment of Fe ions changes the chemistry significantly and is not suitable for description of these systems at ambient pressure. The giant coupling of the on-site Fe-magnetic moment with the As-As bonding that we have discovered here may provide a mechanism for the superconductivity. Since earlier electron-phonon (ep) coupling calculations[67] were done ignoring the Fe-moment, our results raise some questions about the validity of these calculations. Currently we are extending such e-ph coupling calculations to magnetic systems using finite-displacement method in which the magnetic response of the system to the atomic motion is treated fully unlike the standard linear-response perturbation theory.

VI. MAGNETIC PHONONS

Whenever a new superconductor is discovered, the first thing to do is to check whether the conventional electron-phonon (e-ph) coupling can explain the observed transition temperature or not. This was also the case for Fe-pnictide superconductors. Early electron-phonon coupling calculations[67] based on standard non-spin polarized perturbation theory indicate that conventional e-ph can not explain the observed high temperature in Fe-pnictide superconductors. The phonon spectrum and its temperature dependence of various 1111 and 122 systems have been also extensively studied by inelastic neutron scattering[68,69,70], inelastic xray scattering[71,72,73] and by nuclear-resonance spectrum which is Fe-specific[74]. These studies did not find any significant changes in the observed phonon spectrum with superconductivity. However some of these measurements indicate features which are not produced in the standard linear-response non-magnetic phonon calculations. For example, Fukuda *at al.*[72] found that the calculated phonon DOS agrees with the experimental spectrum provided that the computed FeAs force constant is reduced by 30%. Similarly, Reznik *et al*[73] recently observed that in $BaFe_2As_2$ system, the A_g As mode is around 20-22 meV while there is no such feature in the calculated spectrum. Similar observations have been made by inelastic neutron scattering[68] where experimetnal DOS has a nice sharp peak around 20 meV while in the calculated spectrum there is nothing in that energy range. In addition to these observations, there is also a recent Fe-isotope measurements where an isotope coefficient of 0.4 is observed[75]. Some anomalous electron-phonon interaction in doped LaOFeAs has been also reported from first-principles calculations[76]. All these studies suggest that it is probably too early to rule out a possible mechanism based on phonon-mediated superconductivity in Fe-pnictide systems.

So far we have shown that the spin-polarized calculations recover from the failure of non-magnetic calculations in terms of lattice parameters and internal atomic coordinates. Here we show that magnetic calculations also resolve the most of the outstanding issues with the observed phonon modes discussed above. Our phonon calculations are done using the plane wave code pwscf within finite displacement technique as described in Ref.77. The advantage of direct finite displacement technique over the standard linear response theory is twofold. The first advantage is that we can do phonon calcula-

TABLE II: The symmetries and energies (in meV) of the optical phonons of LaOFeAS in P4/nmm and Cmma phases. The energies of the IR-active modes are taken from Ref.19. The * indicates a significant disagreement. The details of calculations and the animations of the modes can be found at http://www.ncnr.nist.gov/staff/taner/laofeas

$\Gamma(P4/nmm)$ = 2 A_{1g} (R) + 4 A_{2u}(IR) + 4 E_u (IR) + 4 E_g(R) + 2 B_{1g} (R) $\Gamma(Cmma)$ = 2 A_g (R) + 2 B_{1g} (R) + 4 B_{1u}(IR) + 4 B_{2g}(R) + 4 B_{2u} (IR) + 4 B_{3g}(R) + 4 B_{3u} (IR)												
P4/nmm	Cmma	IR	P4/nmm	Cmma	IR	P4/nmm	Cmma	IR	P4/nmm	Cmma	IR	P4/nmm Cmma IR
E_u 7.3	7.4-7.5	–	A_{2u} 9.9	10.1	12.1	E_g 14.0	14.1-14.2	–	E_g 17.6	17.7-17.8	–	A_{1g} 22.1 22.3 –
A_{1g} 24.9	25.1	–	B_{1g} 26.6	26.9	–	A_{2u} 31.2	31.6	30.9	E_u 33.7	34.0-34.1	33.2	B_{1g} 35.2 35.6 –
E_g 35.6	35.9- 36.1	–	E_u **34.3**	**34.6- 34.7**	**42.0***	A_{2u} 48.6	49.1	53.8	E_g 51.6	51.8-52.6	–	

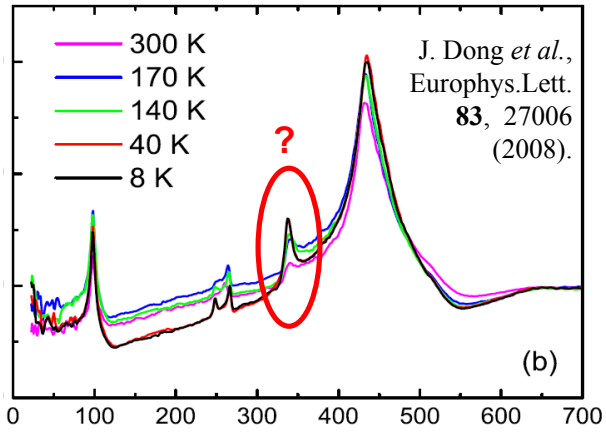

FIG. 16: (color online) The IR data from LaOFEAs sample at different temperatures (adapted from Ref.[19]), indicating very strong temperature dependence for the mode near 340 cm^{-1}, which is calculated . Our calculations do not produce any zone-center phonon near this energy (see Table. 2).

tions with different atomic displacements (usually, 0.01, 0.02, and 0.04 Å) and determine if there is any anharmonic phonons. For harmonic phonons, the results do not depend on the magnitude of the displacement. The second and probably the most important advantage is that we treat the magnetism and phonon displacements equally and self consistently. We have already seen that Fe-magnetic moment is very sensitive to the As-z position and therefore it is not a good approximation to assume that the spins are fixed as the atoms move according to a given phonon mode. In our approach, this direct and strong interplay of magnetism and structure is treated self consistently.

We first discuss the phonon spectrum of 1111 system (i.e. LaOFeAs) in the high (i.e. paramagnetic) and low temperature phases and make some comparison with available IR-data which is shown in Fig. 16. Since in the low-T phase, we have both magnetic ordering and tetragonal-orthorhombic structural phase transition, it is instructive to study the effect of magnetic ordering and structural distortion separately. Hence, we first ignore the Fe-magnetism and consider phonon spectrum when the system is non-magnetic with tetragonal and orthorhombic lattice parameters. Our results are summarized in Table 2. From the the symmetry decomposition of the optical phonons in both P4/nmm and Cmma phases, we note that the distortion does not introduce any new IR active modes but rather just splits the doubly-degenerate modes into non-degenerate ones. However the splitting is quite small; the largest is around 0.2 meV. This explains why no new modes appear in the optical measurements after the transition. We also note that the agreement for the energies of the zone center phonons with IR data is not as good as one expects. In particular, the E_u mode observed at 42 meV is calculated to be 35 meV, a significantly lower value. Interestingly, this particular mode has a strong temperature dependence[19] as shown in Fig. 16. This raises some red flags about the possibility of anharmonic phonons in these systems.

Since the As-z position and the Fe-magnetic moment are tightly coupled, one may naively expect that the c-polarized As A_g mode could be quite anharmonic if we perform magnetic calculations. We have checked this first by performing a frozen-phonon type calculation where we calculate the total energy as the As-atoms are displaced along c-axis in LaOFeAs system (see Fig. 17). Please note that this is not true A_g mode where both As and La atoms are allowed to move along c-axis. We will discuss the full phonon calculations next. Figure 17 shows that the total energy versus the As-displacement can be fit to quadratic equation quite well, suggesting this phonon is harmonic. What is interesting is that the non-spin polarized and spin-polarized calculations give very different harmonic force constants. Including Fe-spin in the calculations softens the force constant by about 20%, consistent with Fukuda's observation[72] that one has to soften the FeAs-force constant to get better agreement with the data. However as we shall see below, the renormalization of the force constants with Fe-spin polarization is quite complicated; almost all of the force constants involving Fe and As are basically renormalized.

We next check if there are other modes in LaOFeAs system that could be anharmonic. We have carried out full spin polarized phonon calculations (gamma point of the $\sqrt{2} \times \sqrt{2}$ cell) with atomic displacements of 0.02 Å and 0.04 Å, respectively. The mode energies are plotted in Fig. 18 for both displacements. It is clear that two

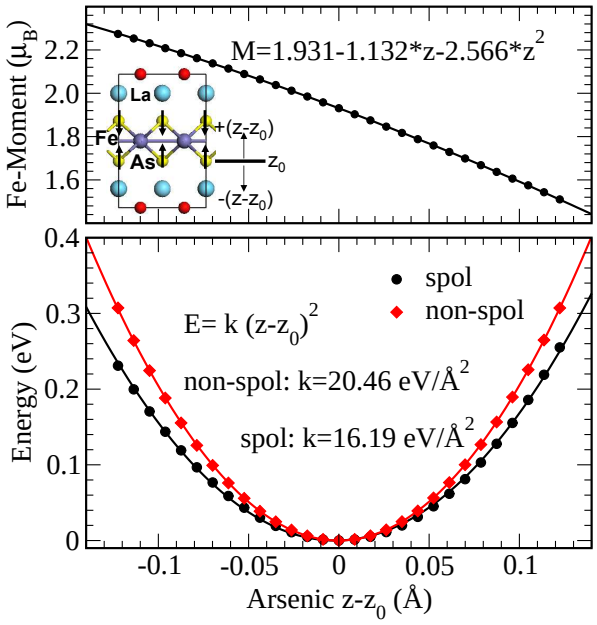

FIG. 17: (color online) Fe-moment and total Energy as As ions are translated along the c-axis as shown in the inset. Note that +(z-z0) corresponds to As ions moving towards the Fe-plane (z0=0.36). Bottom panel indicates that the frozen-phonon potential is harmonic and softens about 20% with spin-polarization.

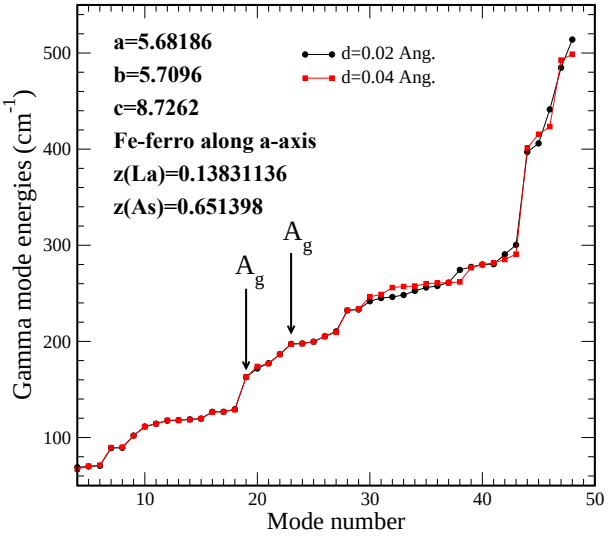

FIG. 18: (color online) Phonon mode energies versus mode numbers from finite-displacement phonon calculations with two different displacements, indicating that most of the phonons are harmonic. There are some modes with very small anharmonicity around 250 cm^{-1} which correspond to Fe-Fe stretching modes. The As c-polarized modes with A_g symmetry are indicated. These modes are harmonic, consisting with frozen-phonon energy plot shown in Fig. 17.

As A_g modes are harmonic. There is some anharmonicity around 250-300 cm^{-1} corresponding to in-plane Fe-Fe stretching modes. However this type of mode energy dependence on the atomic displacement is typical and does not indicate unusual anharmonicity. Hence, we conclude that in Fe-Pnictide system the phonon spectrum is harmonic. This is quite opposite to what we have in MgB_2 superconductor[78] where the in-plane E_{2g} B-B stretching mode was found very anharmonic and responsible for the most of the e-ph coupling[78].

We now discuss the effect of the Fe-spin state on phonon modes in LaOFeAs. Our results are also very similar to 122 systems (in fact the effect of the Fe-spin is more pronounced in 122 systems than in 1111 systems due to strong inter-plane As-As interactions as discussed above). We have carried out three different phonon calculations. In the first two, we ignore Fe-magnetism and just consider tetragonal (i.e. P4/nmm) and primitive cell of the orthorhombic space group Cmma (i.e. P2/c). The third calculation is fully spin-polarized with the orthorhombic cell parameters. We note that when iron spins are considered, the space group of the SDW ordered system is no longer Cmma as reported in neutron experiments[14]. Cmma is the space group of the non-magnetic orthorhombic cell. In our phonon calculations this is a very important point since we use only symmetry independent displacements to construct the dynamical matrix. Using wrong space group, such as Cmma, could average out the anisotropic force constants due to SDW ordering and give wrong results. We determine that the true space group of LaOFeAs when iron spin is considered is Pbmb (spg. number=49, origin 1, a-cb). We note that even this space group is an approximate since we assume that FeAs planes are ordered ferromagnetically along c-axis while they are actually ordered antiferromagnetically. However we checked that the energy difference between ferro and antiferro ordering of the FeAs-planes is too small to have any significant effect on the calculated phonon spectrum (see $J_\perp$ in Fig. 12 for La111). Our results from these three calculations are shown in Fig. 19 and Fig. 20.

Fig. 19 shows how the Arsenic c-polarized A_g mode is effected by the structural and magnetic ordering. We note that due the LaO-plane in 1111 system, we have two A_g modes. In the first one As- and La-atoms move along c-axis in phase. In the second one As and La atoms move opposite (i.e. out-of-phase) along the c-axis. Hence in the out-of-phase A_g mode, the As-La distance changes as the atoms move. This causes the out-of-phase A_g mode to have slightly higher energy than in-phase mode. We also note that As atoms move twice more than La atoms in the in-phase mode. This is reversed in the out-of-phase mode. Because of this difference, the effect of the Fe-spin state is small on the out-of-phase mode. The in-phase A_g mode energy is soften by about 10% from 22.3 meV to 20.18 meV with the iron spin. This is significant and indicates large magneto-elastic interactions in these systems as we have already seen in the case of $CaFe_2As_2$.

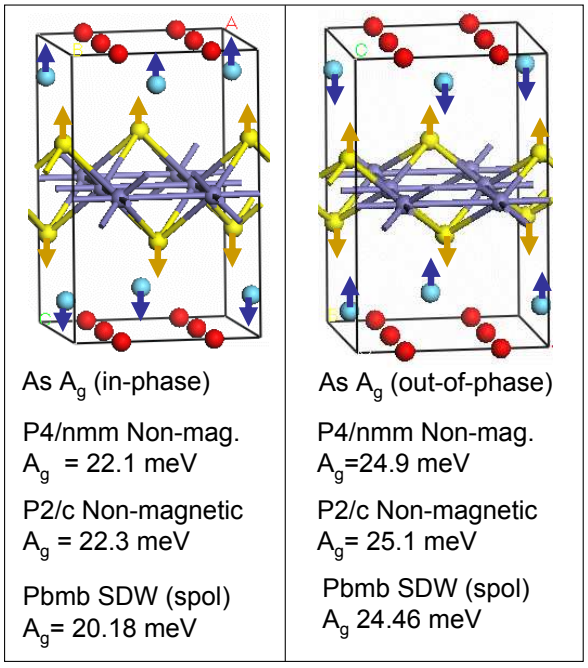

FIG. 19: (color online) Top panel shows two Arsenic c-polarized A_g modes, which are in-phase and out-of-phase with respect to As and La motions along c-axis. The bottom panel shows the mode energies for non-magnetic tetragonal (P4/nmm), non-magnetic orthorhombic distorted lattices (P2/c), and SDW magnetic configuration (Pbmb).

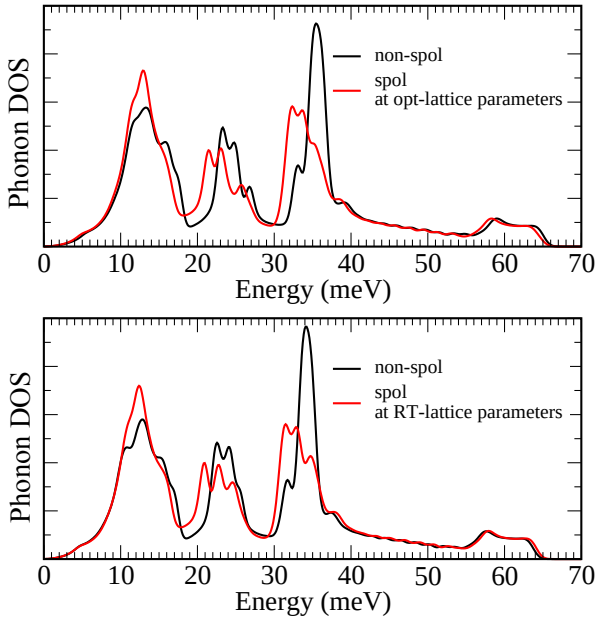

FIG. 20: (color online) Phonon DOS at optimized orthorhombic cell (top) and room-temperature tetragonal cell (bottom) for non-spin polarized (black) and spin-polarized (red) cases. Note that for non-spol case, we have an intense peak at around 34-35 meV. This intense peak is due to oxygen c-polarized phonons (35.50 meV) and oxygen in-plane phonons (34.76 meV) as well as Fe-Fe in-plane stretching mode (34.88 meV) and a mixed As c-polarized mode. When spin-polarization is included all modes associated with Fe-Fe stretching and As c-modes soften and go down to lower energies.

The effect of the spin-polarization on the whole phonon spectrum is shown Fig. 20. The phonon density of states are obtained by calculating the dynamical matrix in a $2\sqrt{2}\times 2\sqrt{2}$ supercell with and without spin-polarization. The effect of the Fe-spin on the phonon DOS is significant. As we have already seen, the first effect is softening the in-phase As A_g c-polarized mode from 22 meV to 20 meV. The 2nd largest effect occurs near the 36 meV energy range. In the non-spin polarized calculations, we obtain very strong and sharp feature near 36 meV, inconsistent with the experimental data. This sharp feature near 35-36 meV is combination of several modes which are both c-polarized and in-plane oxygen and Fe-Fe modes. When we have the Fe-spin included in the calculations, we soften those modes that involve Fe-Fe stretching by about %10, bringing the Fe-modes down to 32 meV where the experimental features are observed.

We also checked the real-space force constants obtained from both spin-polarized and non-magnetic calculations. While La and O onsite force constants are not effected with Fe-spin, the onsite Fe and As force constants are renormalized by about 10-20%. For example, the non-spin polarized case gives force constants (in eV/$\AA^2$) (11.06,11.06,8.7) for Fe and (10.48, 10.50, 9.33) for As, respectively. The spin-polarized calculations renormalize these force constants to (10.8, 8.5, 8.5) for Fe and (9.2,8.8, 8.6) for As. The change in the force constants are significant. We also observe similar softening up to 20% in the Fe-As and Fe-Fe force constants. Hence the 10% phonon softening of the As A_g mode and Fe-Fe stretching modes near 35 meV is due to complicated renormalization of the force constants rather than a simple rescaling of a single force constant as suggested by Futuda *et al.*[72]. The important point is that Fe-spin is needed to get the observed spectrum even though the measurements are done on samples at temperatures well above the T_N.

Fig.20 also shows that using room temperature or optimized lattice parameters gives only slightly different phonon spectrum. This is consistent with the observed weak temperature dependence of the neutron or inelastic x-ray data. Of course, in reality there is a huge difference between the room temperature and low temperature calculations if we ignore the Fe-magnetism at room temperature and consider it at low temperature.

We will finish this section by presenting phonon spectrum of $Ba_{0.5}K_{0.5}Fe_2As_2$ for which the difference between non-magnetic and magnetic DOS is huge as expected from our previous work on $CaFe_2As_2$ due to strong As-As interactions. In Fig. 21 we compare our calculated phonon DOS with the neutron data of Zbiri *et al.*[68] on $BaFe_2As_2$ sample. The authors indicated that a peak near 20 meV can not be produced from non-spin polarized calculations. Zbiri's neutron data shown in Fig. 21 is fully consistent with the recent inelastic X-ray study

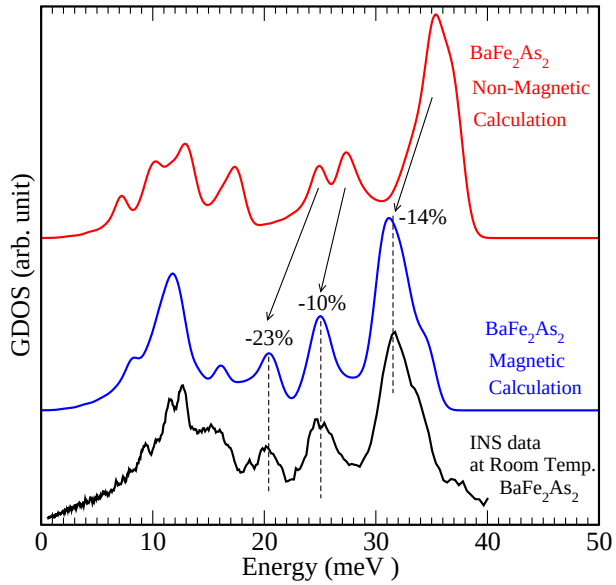

FIG. 21: (color online) Generalized Phonon DOS measured by inelastic neutron scattering at room temperature for $BaFe_2As_2$ (bottom black curve)[68] and the calculated GDOS with (middle blue) and without (top red) Fe-magnetism. Note that including Fe-spin in the calculations softens the Fe-Fe in-plane and As c-phonons by about %10 and %23 and results a DOS that is in perfect agreement with the room temperature data (i.e well above $T_N = 140$ K).

of Reznik *et al.*[73]. They have also measure c-polarized As dispersion mode near 20-22 meV but their non-spin polarized calculations did not produce any peak in the energy range of 20-26 meV[73]. Zbiri *et al.* called this energy range as "pseudo-gap" in the phonon spectrum since in the dispersion curves there are no modes in this energy range that can give a sharp peak in the DOS. In Fig. 21 we show that considering magnetic phonons again solves all the mysterious! Our non-magnetic phonon calculations are in good agreement with Reznik phonon dispersion curve[73] as well as Zbiri's results[68] and therefore it can not explain the observed GDOS of $BaFe_2As_2$. However our magnetic phonon calculations soften the c-polarized As mode by 23% and the Fe-Fe modes by about %10-14, respectively. Hence the magnetic phonon DOS is now in perfect agreement with the experimental data. This further supports our theory that Fe-magnetism always present in Fe-pnictide systems even at temperatures well above T_N. The iron magnetism could be in the form of fluctuating SDW type small magnetic domains[79] or it could be at the atomic limit of paramagnetic Fe ions (i.e. para-magnon). More study is needed to have a better understanding of the Fe-magnetism in these systems. From the results presented here it is clear that iron-magnetism in the Fe-pnictides is the key factor that controls atomic positions, lattice parameters, structural phase transition, phonon energies, and most probably the superconducting properties as well.

VII. CONCLUSIONS

Our conclusions can be summarized as follows:

- Accurate all-electron fix-spin total energy calculations indicate that the ferromagnetic and checkerboard antiferromagnetic ordering in Fe-pnictides were not stable and the stripe Fe-spin configuration (i.e. SDW) is the only stable ground state. Mapping the energies of ferromagnetic, checkerboard AF and SDW spin configurations on to an approximate J_1^a-J_1^b-J_2 model indicates the presence of competing strong antiferromagnetic exchange interactions in these systems. This suggests that magnetism and superconductivity in doped Fe-pnictides may be strongly coupled, much like in the high-T_c cuprates.

- The magnetic stripe SDW phase breaks the tetragonal symmetry, removes the frustration, and causes a structural distortion. A simple model based on spin-Peierls like transition (i.e. the lattice parameters dependence of the exchange constants J_1 and J_2) is shown to give the correct amount of lattice distortion as well as predicts the fine details such as in SDW ordering parallel aligned spin-direction gets shorter while the anti-parallel aligned spin direction gets longer. We show that the structural transition temperature, T_{str} does not correlate with FeAs-inter-plane magnetic interaction $J_\perp$. The coupling of the magnetic fluctuations to the in-plane strains $\epsilon_{xx} - \epsilon_{yy}$ and occupations of orbitals $d_{xz} - d_{yz}$ may change the nature of magnetic transition to first order and splits the magnetic and structural ordering temperatures depending on the details of the system[59,60,61,62,63].

- The magnetic exchange interactions $J_{i,j}(R)$ are calculated as a function of Fe-Fe distance R from two totally different approaches. Both methods indicate that the exchange interactions along the Fe-Fe square-diagonal spin-direction are short range and antiferromagnetic. Hence it is tempting to conclude that the main diagonal interaction, J_2 is superexchange type and important contributer towards the stabilization of SDW ordering. Along the parallel and antiparallel aligned spin-directions, however, the exchange interactions have oscillatory character with an envelop decaying as $1/R^3$, just like in bcc-Fe. The major difference between two methods is that the first nearest-neighbor exchange interaction along the parallel spin direction is found to be antiferromagnetic in spin-flip method and ferromagnetic in linear-response theory. Assuming both methods are accurate, this implies that a simple Heisenberg model is not appropriate for the Fe-pnictide systems (see Fig. 5). However for a given orbital order and spin-configuration, one can still

use it to describe the low-energy excitations such as spin-waves.

Since the spin-flip method is more appropriate at high temperatures above the magnetic phase transition, we obtain results that are close to paramagnetic tetragonal symmetry (i.e. $J_1^a \approx J_1^b$) and the system is fully frustrated. As the system orders, the occupancy of the d_{xz} start differ from the occupancy of d_{yz} orbital, giving rise to orbital-dependent exchange spin-interactions. At low temperatures where spin-wave approximation is valid, the exchange interaction along the stripe direction becomes weak and ferromagnetic. At this point, the spin-frustration is totally removed (i.e. all magnetic bonds are satisfied). Hence, it would be very interesting to determine the exchange interactions and their temperature dependence by inelastic neutron scattering measurements. We gave a brief discussion about how the spin-wave spectrum would appear from a single crystal sample with orthorhombic twinning. Due to large anisotropy of the spin-wave velocities within the ab-plane, it may be possible to resolve the spin waves along the a and b directions and determine the sign of the J_1^b exchange interaction despite the orthorhombic twinning.

- We unravel surprisingly strong interactions between arsenic ions in Fe-pnictides, the strength of which is controlled by the Fe-spin state in an unprecedented way. Reducing the Fe-magnetic moment, weakens the Fe-As bonding, and in turn, increases As-As interactions, causing a giant reduction in the c-axis. For $CaFe_2As_2$ system, this reduction of c-axis with the loss of the Fe-moment is as large as 1.4 Å, an unheard of giant coupling of local spin-state of an ion to its lattice. Since the calculated large c-reduction has been recently observed only under high-pressure, our results suggest that the iron magnetic moment should be present in Fe-pnictides at all times at ambient pressure.

- Finally, we showed that Fe-magnetism is also the key in understanding the phonons in Fe-pnictides. Our magnetic phonon calculations clearly indicate that the observed phonon-DOS at room temperature is much closer to the calculated magnetic phonon-DOS rather than non-magnetic one. We find that the in-plane Fe-Fe and c-polarized As phonon modes are soften by about %23 and %10 for 122 and 1111 systems, respectively, explaining the observed inealastic x-ray data by Fukuda *et al.*[72] and by Reznik *et al.*[73], and the INS room temperature GDOS data on $BaFe_2As_2$ by Zbiri *et al*[68]. This finding further supports our theory that the Fe-magnetism must present in these systems all the time.

- The main conclusion of our work is that there is a giant magneto-elastic coupling in Fe-pnictides. We can successfully predict lattice parameters, atomic positions and phonons in these systems from first principles provided that we always consider Fe-spin in our calculations. Since the current electron-phonon calculations were carried out without the Fe-spin, it is probably too early to rule out el-phonon coupling as a possible mechanism. It is very important that electron-phonon coupling is calculated self-consistently with the Fe-spin and without the rigid-spin approximation since Fe-moment is very sensitive to arsenic motion. Currently we are carrying out such calculations and the results will be presented elsewhere.

VIII. ACKNOWLEDGMENTS

The author acknowledges fruitful discussions with P. Dai, A. B. Harris, J. W. Lynn, I. I. Mazin, and W. Ratcliff.

APPENDIX A: EXCHANGE INTERACTIONS FROM DIRECT SPIN-FLIP METHOD IN A LARGE SUPERCELL

We developed a systematic approach where the exchange parameter between spin-i and spin-j is obtained from the total energies of a reference magnetic configuration and those configurations obtained by flipping the spins i and j one at a time and simultaneous flipping of both spins. From these four energies, it is possible to obtain the exchange constant between spin i and j. We note that here we are interested in the isotropic exchange interactions. We also do not consider spin-orbit interactions in our calculations. Hence all calculations are done for collinear spin-configurations.

In order to extract superexchange interactions up to a large cutoff distance, we calculated the total energy for various periodic spin configurations based on SDW alignment of the z-components of spin ($S_z = \pm 1$) with a $3\sqrt{(}2) \times 3\sqrt{2}$ supercell of the LaOFeAs which contains 144 atoms (36 of which are Fe ions). Since the spin configuration is the same from one supercell to the next one we may write the total energy E_1 as

$$\begin{aligned} E_1 &= E_0 + \frac{1}{2}\sum_{\mathbf{R}}\sum_{k,l} J(0,k;\mathbf{R},l) S_k(0) S_l(\mathbf{R}) \\ &= E_0 + \frac{1}{2}\sum_{k,l} K(k,l) S_k S_l \ , \end{aligned} \tag{A1}$$

where $S(n,\mathbf{R}) \equiv S_n$ is the spin of the nth ion in the supercell at $\mathbf{R}$ and because of periodicity $K(k,l) = K(l,k) \equiv \sum_{\mathbf{R}} J(k,0;l,\mathbf{R})$. It is obvious that we can only expect to determine $K(k,l)$ and not the individual J's. However, since the supercell is reasonably large, we

can identify the K's with the J at the minimal separation. It is also obvious that we can only hope to determine $K(i,j)$ for $i \neq j$, since the energy involving $K(i,i)$ depends on $(S_i)^2 = 1$ since $S_i = \pm 1$ for Ni spins. To determine $K(i,j)$ for $i \neq j$ we calculate four total energies, E_1 and the other three corresponding energies when we independently change the sign of S_i and S_j. When we change the sign of S_i we get

$$E_2 \;=\; E_0 + \frac{1}{2}\sum_{k,l} K(k,l) S_k [1 - 2\delta_{i,k}] S_l [1 - 2\delta_{i,l}] \quad \text{(A2)}$$

where $\delta_{n,m} = 1$ if $n = m$ and is zero otherwise. Likewise when we change the sign of S_j we get

$$E_3 \;=\; E_0 + \frac{1}{2}\sum_{k,l} K(k,l) S_k [1 - 2\delta_{j,k}] S_l [1 - 2\delta_{j,l}] \quad \text{(A3)}$$

and when we change the sign of both spins i and j we get

$$E_4 = E_0 + \frac{1}{2}\sum_{k,l} \quad K(k,l) S_k [1 - 2\delta_{i,k}][1 - 2\delta_{j,k}] S_l \times [1 - 2\delta_{i,l}][1 - 2\delta_{j,l}] \; . \quad \text{(A4)}$$

Then we construct the quantity $X = E_1 - E_2 - E_3 + E_4$, to get

$$X = \frac{1}{2}\sum_{k,l} K(k,l) S_k S_l \quad [2\delta_{i,k} + 2\delta_{i,l} - 4\delta_{i,k}\delta_{i,l}] \times [2\delta_{j,k} + 2\delta_{j,l} - 4\delta_{j,k}\delta_{j,l}] \quad \text{(A5)}$$

Since we require that $i \neq j$, this gives

$$X \;=\; 4K(i,j) S_i S_j \; , \quad \text{(A6)}$$

from which we can extract the value of $K(i,j)$. If the supercell is large enough, one can keep only the interactions between the nearest neighboring supercell images of the spins and therefore the calculated exchange parameter can be attributed to spin-interaction between the closest pairs of spins of types i and j. We also note that there are cases where spin j is at the mid-point between spin $S_i(0)$ and one of its images at $S_i(\mathbf{R})$. In that case, the calculated superexchange constant is twice of the $J_{i,j}$. Similarly there are cases where the spin j is at a point where it interacts equally with four images of the spin i. In those cases, the calculated J is four times $J_{i,j}$.

* Electronic address: taner@nist.gov

1 Y. Kamihara, T. Watanabe, M Hirano, H. Hosono, J. Am. Chem. Soc. **130**, 3296 (2008).
2 X. H. Chen, *et al*, Nature **453**, 761 (2008).
3 G. F. Chen *et al.*, Phys. Rev. Lett. **100**, 247002 (2008).
4 Z. A. Ren, Materials Research Innovations **12**, 105 (2008); also cond-mat:0803.4283v1 (2008).
5 C. Krellner *et al.*, Phys. Rev. B **78**, 100504(R) (2008).
6 A. Jesche, *et al.*, Phys. Rev. B **78**, 180504(R) (2008).
7 A. I. Goldman *et al.*, Phys. Rev. B **78**, 100506(R) (2008).
8 J. Zhao *et al.*, Phys. Rev. B **78**, 140504(R) (2008).
9 Q. Huang *et al.*, Phys. Rev. Lett. **101**, 257003 (2008).
10 X. C. Wang *et al.*, Solid State Commun. **148**, 538 (2008).
11 M. H. Fang, Phys. Rev. B **78**, 224503 (2008)
12 D. J. Singh, arXiv:091.2149 (2009).
13 I. I. Mazin and J. Schmalian, arXiv:0901.4790 (2009).
14 Jeffrey W. Lynn and Pengcheng Dai, arXiv:0902.0091 (2009).
15 C. de la Cruz, Q. Huang, J. W. Lynn, J. Li, W. Ratcliff II, H. A. Mook, G. F. Chen, J. L. Luo, N. L. Wang, and Pengcheng Dai, *Nature* **453**, 899 (2008).
16 H.-H. Klauss, *et al.*, Phys. Rev. Lett. **101**, 077005 (2008).
17 D. J. Singh and M.-H. Du, Phys. Rev. Lett. **100**, 237003 (2008).
18 S. Ishibashi, K. Terakura, and H. Hosono, J. Phys. Soc. Jpn. **77**, 053709 (2008).
19 J. Dong *et al.*, Euro. Phys. Lett. **83**, 27006 (2008).
20 I. I. Mazin, D. J. Singh, M. D. Johannes, and M. H. Du, Phys. Rev. Lett. **101**, 057003 (2008).
21 T. Yildirim, Phys. Rev. Lett. **101**, 057010 (2008).
22 G. Wu *et al.*, J. Phys. Condens. Matter **20**, 422201 (2008).
23 H. H. Wen, G. Mu, L. Fang, H. Yang, and X. Y. E. Zhu, Euro. Phys. Lett. **82**, 17009 (2008).
24 G. F. Chen *et al.*, Chin. Phys. Lett. **25**, 3403 (2008); also arXiv:0806.1209 (2008)
25 K. Sasmal *et al.*, Phys. Rev. Lett. **101**, 107007 (2008).
26 T. Park *et al.*, J. Phys. Condens. Matter **20**, 322204 (2008).
27 P. L. Alireza *et al.*, J. Phys. Condens. Matter **21**, 012208 (2008).
28 N. Ni *et al.*, A. Kreyssig, A. I. Goldman, E. D. Mun, S. L. Bud'ko, P. C. Canfield, Phys. Rev. B **78**, 014523 (2008).
29 T. Nomura *et al.*, Supercond. Sci. Technol. **21** 125028 (2008).
30 Gang Xu *et al.*, Europhysics Letters **82**, 67002 (2008).
31 K. Haule, J. H. Shim, G. Kotliar, cond-mat:0803.3236 (2008).
32 F. Ma, Z.Y. Lu, and T. Xiang, Phys. Rev. B **78**, 224517 (2008).
33 C. Cao, P. J. Hirschfeld, and H. P. Cheng, Phys. Rev. B **77**, 220506(R) (2008).
34 Z. P. Yin, S. Lebgue, M. J. Han, B. Neal, S. Y. Savrasov, and W. E. Pickett, Phys. Rev. Lett. **101**, 047001 (2008).
35 I. I. Mazin, M. D. Johannes, L. Boeri, K. Koepernik, D. J. Singh, Phys. Rev. B **78**, 085104 (2009).
36 S. Lebegue, Z. P. Yin, and W. E. Pickett, New Journal of Physics, special issue of iron-based superconductors (arXiv:0810.0376, 2008).
37 T. Yildirim, A. B. Harris, and E. F. Shender, Phys. Rev. B **53**, 6455 (1996).
38 S. H. Lee, C. Broholm, T. H. Kim, W. Ratcliff II, and S-W. Cheong, Nature **453**, 899 (2008). Phys. Rev. Lett. **84**, 3718 (2000).
39 A. N. Yaresko, G.-Q. Liu, V. N. Antonov, and O. K. Andersen, arXiv:0810.4469 (2009).

[40] P. Blaha, K. Schwarz, P. Sorantin, and S. B. Trickey, Comput. Phys. Commun. **59**, 339 (1990).
[41] http://exciting.sourceforge.net/
[42] http://www.pwscf.org
[43] Q. Si and E. Abrahams, Phys. Rev. Lett. **101**, 076401 (2008).
[44] J. Wu, P. Philips, and A. H. C. Neto, Phys. Rev. Lett. **101**, 126401 (2008).
[45] J. C. Wojde, I. P. R. Moreira, and F. Illlas, J. Am. Chem. Soc. **131**, 906 (2009).
[46] M. J. Han, Q. Yin, W. E. Pickett, and S. Y. Savrasov, Phys. Rev. Lett., in press (2009); also arXiv:0811.0034 (2008).
[47] K. D. Belashchenko and V. P. Antropov, Phys. Rev. B **78**, 212505 (2008).
[48] E. Manousakis, J. Ren, S. Meng, and E. Kaxiras, Phys. Rev. B **78**, 205112 (2008).
[49] F. Kruger, S. Kumar, J. Zaanen, and J. van den Brink, arXiv:0811.4104 (2008).
[50] J. Zhao *et al.*, Phys. Rev. Lett. **101**, 167203 (2008).
[51] R. A. Ewings *et al.*, Phys. Rev. B **78**, 220501 (R) (2008).
[52] R. J. McQueeney *et al.*, Phys. Rev. Lett. **101**, 227205 (2008)
[53] S. O. Diallo *et al.*, arXiv:0901.3784 (2009)
[54] M. J. Han, T. Ozaki, and J. Yu, Phys. Rev. B **70**, 184421 (2004).
[55] A. I. Liechtenstein, M. I. Katsnelson, V. P. Antropov, and V. A. Gubanov, J. Magnetism and Magnetic Materials **67**, 65 (1987).
[56] M. Pajda, J. Kudrnovsky, I. Turek, V. Drchal, and P. Bruno, Phys. Rev. B **64**, 174402 (2001).
[57] T. Ozaki, openmx package: http://www.openmx-square.org/
[58] K. Kaneko *et al.*, Phys. Rev. B **78**, 212502 (2008).
[59] A. B. Harris and T. Yildirim, to be published (2009).
[60] C. Xu, M. Muller, and S. Sachdev, Phys. Rev. B **78**, 020501(R) (2008).
[61] C. Fang, H. Yao, W.F. Tsai, J. Hu, and S. A. Kovelson, Phys. Rev. B **77**, 224509 (2008).
[62] K. Sun, B. M. Fregoso, M. J. Lawler, and E. Fradkin, Phys. Rev. B **78**, 085124 (2008).
[63] V. Barzykin and L. P. Gor'kov, arXiv:0812.4277 (2008).
[64] A. Kreyssig *et al.*, Phys. Rev. B **78**, 184517 (2008).
[65] T. Yildirim, Phys. Rev. Lett. **102**, 037003 (2009).
[66] M. S. Torikachvili *et al.*, Phys. Rev. Lett. **101**, 057006 (2008).
[67] L. Boeri, O. V. Dolgov, and A. A. Golubov, Phys. Rev. Lett. **101**, 026403 (2008).
[68] M. Zbiri, H. Schober, M. R. Johnson, S. Rols, R. Mittal, Y. Su, M. Rotter, D. Johrendt, Phys. Rev. B **79**, 064511 (2009).
[69] A. D. Christianson *et al.* Phys. Rev. Lett. **101**, 157004 (2008).
[70] Y. Qiu, M. Kofu, W. Bao, S.-H. Lee, Q. Huang, T. Yildirim, J. R. D. Copley, J. W. Lynn, T. Wu, G. Wu, and X. H. Chen, Phys. Rev. B **78**, 052508 (2008).
[71] M. Le. Tacon, M. Krisch, A. Bosak, J.-W.G. Bos, and S. Margadonna, arXiv:0809.2898 (2008).
[72] T. Fukuda *et al.*, J. Phys. Soc. Jpn. **77**, 103715 (2008).
[73] D. Reznik *et al.*, arXiv:0810.4941 (2008).
[74] S. Higashitaniguchi *et al.*, Phys. Rev. B **78**, 174507 (2008).
[75] R. H. Liu, T. Wu, G. Wu, H. Chen, X. F. Wang, Y. L. Xie, J. J. Yin, Y. J. Yan, Q. J. Li, B. C. Shi, W. S. Chu, Z. Y. Wu, and X. H. Chen, arXiv: 0810.2694 (2008).
[76] F. Yndurain and J. M. Soler, arXiv:0810.2474 (2008).
[77] T. Yildirim, Chem. Phys. **261**, 205 (2000).
[78] T. Yildirim *et al.*, Phys. Rev. Lett. **87**, 037001 (2001).
[79] I. I. Mazin and M. D. Johannes, Nature Physics **5**, 141 (2009).